

¹ New isolate genomes and global marine ² metagenomes resolve ecologically ³ relevant units of SAR11

⁴

⁵ Kelle C. Freel¹, Sarah J. Tucker^{1,2,3,4,5}, Evan B. Freel¹, Stephen J. Giovannoni⁶, A. Murat

⁶ Eren,^{3,4,5,7,8}, & Michael S. Rappé^{1*}

⁷

⁸ ¹Hawai‘i Institute of Marine Biology, University of Hawai‘i at Mānoa, Kāne‘ohe, Hawai‘i,

⁹ United States; ²Marine Biology Graduate Program, University of Hawai‘i at Mānoa, Honolulu,

¹⁰ Hawai‘i, United States; ³Josephine Bay Paul Center for Comparative Molecular Biology and

¹¹ Evolution, Marine Biological Laboratory, Woods Hole, MA 02543, USA; ⁴Helmholtz Institute

¹² for Functional Marine Biodiversity, 26129 Oldenburg, Germany; ⁵Alfred Wegener Institute,

¹³ Helmholtz Centre for Polar and Marine Research, 27570 Bremerhaven, Germany; ⁶Department

¹⁴ of Microbiology, Oregon State University, 97331 Corvallis, OR, United States; ⁷Institute for

¹⁵ Chemistry and Biology of the Marine Environment, University of Oldenburg, 26129 Oldenburg,

¹⁶ Germany; ⁸Max Planck Institute for Marine Microbiology, 28359 Bremen, Germany

¹⁷

¹⁸ *Corresponding Author. Email: rappe@hawaii.edu

¹⁹ Running Title: SAR11 genomes from the tropical Pacific

²⁰

21 Abstract

22 The bacterial order *Pelagibacterales* (SAR11) is among the most abundant and widely
23 distributed microbial lineages across the global surface ocean, where it forms an integral
24 component of the marine carbon cycle. However, the limited availability of high-quality
25 genomes has hampered comprehensive insights into the ecology and evolutionary history of this
26 critical group. Here, we increase the number of complete SAR11 isolate genomes fourfold by
27 describing 81 new SAR11 strains from seven distinct lineages isolated from coastal and offshore
28 surface seawater of the tropical Pacific Ocean. We leveraged comprehensive phylogenomic
29 insights afforded by these isolates to characterize 24 monophyletic, discrete ecotypes with unique
30 spatiotemporal patterns of distribution across the global ocean, which we define as genera. Our
31 data illustrate fine-scale differentiation in patterns of detection with ecologically-relevant gene
32 content variation for some closely related genomes, demonstrating instances of ecological
33 speciation within SAR11 genera. Our study provides unique insight into complex environmental
34 SAR11 populations, and proposes an ecology-informed hierarchy to pave a path forward for the
35 systematic nomenclature for this clade.

36 Main

37 SAR11 marine bacteria are a genetically diverse, order-level lineage of heterotrophs
38 within the *Alphaproteobacteria* known as the *Pelagibacterales* (Grote et al. 2012) that
39 numerically dominate planktonic communities across the global ocean (Morris et al. 2002;
40 Carlson et al. 2009; Eiler et al. 2009; Schattenhofer et al. 2009; Becker et al. 2019). Associations
41 between the spatiotemporal distribution of operationally defined subclades and environmental
42 variables suggest the presence of distinct ecotypes within SAR11 (Carlson et al. 2009; Eren et al.
43 2013a; Delmont et al. 2019; Tucker et al. 2021). Previous studies further support the functional
44 differentiation of subclades (Grote et al. 2012; Thrash et al. 2014), even across short
45 biogeographical distances (Tucker et al. 2024a). While limited in number, the available
46 high-quality SAR11 genomes have demonstrated that this group is a remarkably cohesive genetic
47 assemblage (Grote et al. 2012), making it an attractive model to study the capacity of a
48 minimalist genome to reach stunning levels of success.

49 Since the first observation of SAR11 through environmental 16S rRNA gene fragments
50 over three decades ago (Giovannoni et al. 1990), microbiology has benefited from a dramatic
51 increase in microbial sequence data recovered directly from the environment, offering
52 representative genomes for many difficult to cultivate microbial lineages (Hug et al. 2016).
53 However, even the most comprehensive genome-resolved surveys of marine metagenomes have
54 failed to yield high-quality SAR11 genomes (Paoli et al. 2022), resulting in limited insights into
55 what constitutes ecologically meaningful units within this broad group. The extensive intra-clade
56 diversity of SAR11 (Tsementzi et al. 2016; Kiefl et al. 2023) confounds the ability to reconstruct

57 environmental genomes from metagenomes (Delmont et al. 2018; Tully et al. 2018), which is
58 why one of the most abundant microbial clades in marine systems suffers from poor
59 representation in genome-resolved metagenomics surveys (Chang et al. 2024). Circumventing
60 the need to assemble complex metagenomes first for genome recovery, single-cell sorting
61 techniques have been much more effective in sampling environmental SAR11 populations
62 through single-amplified genomes (SAGs). However, in an extensive effort to characterize
63 surface ocean microbes, the estimated genome completion of SAGs that could be affiliated with
64 SAR11 remained below 60% (Pachiadaki et al. 2019), a level that prevents robust phylogenomic
65 insights. Such barriers have led to a reliance on isolate genomes to investigate the evolution of
66 SAR11 populations (Vergin et al. 2007; Wilhelm et al. 2007; Thrash et al. 2011; Grote et al.
67 2012; Muñoz-Gómez et al. 2019), yet following this path has been impeded by another
68 formidable challenge: the difficulty of cultivating SAR11 in the laboratory, even with genomic
69 insights regarding its unique growth requirements (Tripp et al. 2008; Carini et al. 2013; Sun et al.
70 2016).

71 The first successful cultivation of SAR11 in 2002 resulted in the isolation of *Pelagibacter*
72 *ubique* strain HTCC1062 (Rappé et al. 2002), followed by the publication of its complete
73 genome (Giovannoni et al. 2005). Over the past two decades, additional isolate genomes have
74 been few, with only 25 currently available. Despite their rarity, high-quality genomes from
75 isolated strains not only shed light on SAR11 biology (Schwalbach et al. 2010; Sun et al. 2011;
76 Carini et al. 2013) and the origins of this lineage within the *Alphaproteobacteria* (Thrash et al.
77 2011; Grote et al. 2012; Muñoz-Gómez et al. 2019), but also have made it possible to establish
78 key concepts in biology such as genome streamlining (Schwalbach et al. 2010; Sun et al. 2011;

79 Grote et al. 2012; Viklund et al. 2012; Giovannoni et al. 2014; Giovannoni 2017) and investigate
80 the evolutionary processes that shape protein evolution (Delmont et al. 2019; Kiefl et al. 2023).

81 Here we report 81 high-quality genomes from SAR11 strains, increasing the number
82 available for SAR11 isolates by fourfold, and leverage this new collection to build a robust
83 genome phylogeny for the order *Pelagibacterales*. By incorporating publicly available,
84 high-quality single-cell genomes and surface ocean metagenomes from both a steep, nearshore to
85 open-ocean local environmental gradient and elsewhere from around the globe, we reveal
86 cohesive patterns of genomic and ecotypic diversification. We propose a framework through
87 which to characterize and interpret genome heterogeneity at multiple stages along the
88 evolutionary history of SAR11 marine bacteria, and establish a roadmap for future efforts to
89 organize this globally abundant bacterial clade.

90 **Results**

91 **Eighty-one high-quality genomes sequenced from 206 newly isolated SAR11 strains and 92 co-cultures**

93 Three dilution-to-extinction culturing experiments using surface seawater collected from
94 nearshore and adjacent offshore environments of O‘ahu, Hawai‘i, in the tropical Pacific Ocean
95 resulted in 916 isolates from 2,102 inoculated cultures (Table 1; Supplemental Fig. 1). Using a
96 streamlined isolate-to-genome approach, we identified 206 cultures as either pure SAR11 strains
97 or mixed cultures with at least 50% of the total reads matching a SAR11 strain via 16S rRNA
98 gene amplicon sequencing (Supplemental Table 1), and sequenced draft genomes from 90.
99 Manual curation resulted in 79 high-quality SAR11 isolate genomes. The genomes from two

100 strains (HIMB123 and HIMB109) isolated from a previous culture experiment were also added
101 (Brandon 2006), resulting in 81 new SAR11 genomes from isolates. The majority of these
102 (n=60) assembled into ten contigs or less, including 24 closed genomes and an additional 30
103 containing one to three contigs. They ranged from 1.00 to 1.54 Mbp in size and GC content of
104 28.5 to 30.7% (Supplemental Table 2). The median pairwise genome-wide average nucleotide
105 identity (gANI) value across all genomes was 81.8% and none of the 81 new isolate genomes
106 were identical. Having captured a genetically diverse array of SAR11 isolates, we used a
107 phylogenomic approach to characterize evolutionary relationships between these genomes and to
108 high-quality single-cell and isolate genomes previously retrieved from seawater.

109

110 **Table 1. Summary of high-throughput culturing (HTC) experiments.**

111

Site	Inoculum source	Inoculum size (# of cells)	Cultures screened	Positive cultures	SAR11 genomes
SB	raw seawater	5	576	339	53
STO1	raw seawater	5	576	126	16
STO1	cryopreserved seawater	5	480	142	9
STO1	cryopreserved seawater	100	470	343	1

112

113 **A comprehensive genome phylogeny reveals a robust evolutionary backbone populated by
114 clusters of closely related genomes**

115 We first sought to resolve relationships between the strains isolated in this study and
116 other publicly available high-quality *Pelagibacterales* genomes to precisely establish where the
117 new genomes originate from within the broad spectrum of known SAR11 diversity. For this, we
118 created a database that, in addition to the 81 genomes presented here, included 25 public SAR11
119 isolate genomes, 8 of which were also isolated from off the windward coast of O‘ahu, Hawai‘i,
120 and 375 SAR11 single-amplified genomes (SAGs) estimated to be $\geq 85\%$ complete with a

121 redundancy <5% (Supplemental Table 3). We also included five additional SAR11 SAGs of
122 potentially unique evolutionary origin in this collection (Vergin et al. 2013; Thrash et al. 2014),
123 though we excluded genomes from putative SAR11 subgroups IV (Vergin et al. 2013) and V
124 (Thrash et al. 2011) due to their unlikely or, at a minimum, uncertain shared common ancestry
125 with SAR11 (Thrash et al. 2011; Viklund et al. 2013; Haro-Moreno et al. 2020; Muñoz-Gómez et
126 al. 2022). This resulted in a curated collection of 481 SAR11 genomes to assess the evolutionary
127 backbone for SAR11.

128 Previous studies investigating phylogenomic relationships within the
129 *Alphaproteobacteria* utilized a curated set of 200 single-copy core genes (SCGs) for this
130 bacterial class (Wang and Wu 2013; Muñoz-Gómez et al. 2019). We evaluated the presence of
131 these 200 SCGs across our genome dataset, and excluded genes missing in more than 90% of the
132 481 SAR11 genomes. This resulted in a SAR11-specific SCG set of 165 genes for downstream
133 phylogenomic analyses, referred to hereafter as the SAR11_165 core gene set (Supplemental
134 Table 4).

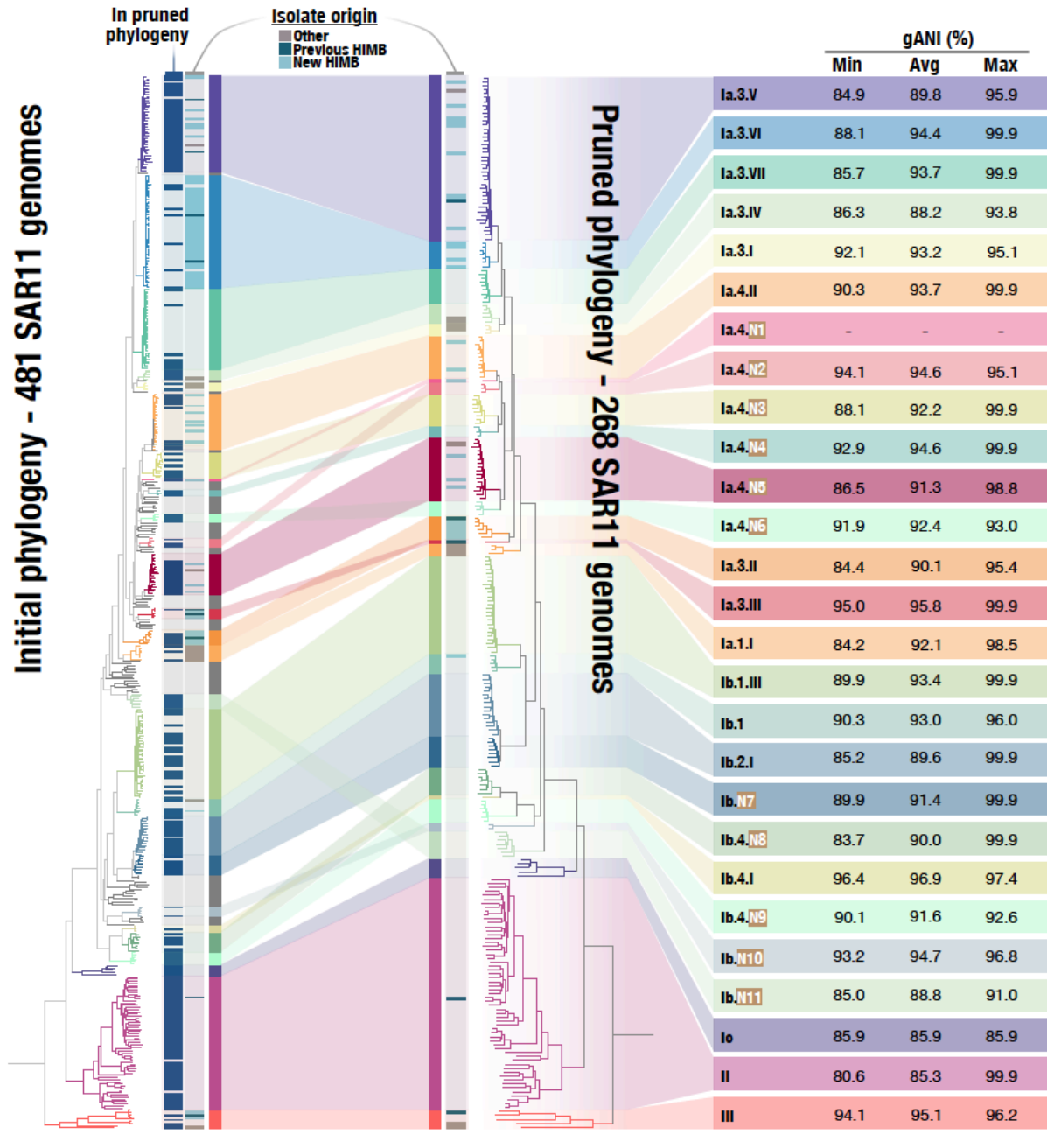
135 Our analysis of the 481 genomes using the SAR11_165 gene set revealed that the SAR11
136 clade consists of four robust, deeply-branching sublineages (Fig. 1; Supplementary Fig. 2). Three
137 of these branches were the previously characterized subclades Ic (Vergin et al. 2013), II (Suzuki
138 et al. 2001), and III (Morris et al. 2005), while the fourth was a combination of established
139 SAR11 subclades Ia and Ib (Suzuki et al. 2001), which did not form separate monophyletic
140 subclades in this comprehensive genomic dataset and robust phylogenetic analysis. If the SAR11
141 clade is assigned to the taxonomic level of a bacterial order, then these four lineages logically
142 resolve to the taxonomic level of families.

143 We further removed genomes from this initial tree in two steps. First we excluded SAGs
144 that did not fall into a 90% gANI cluster of at least three genomes to focus our analyses on
145 well-resolved regions of the tree. Second, we de-replicated the remaining genomes using a
146 conservative cutoff of 95% gANI to minimize subsequent competitive metagenomic recruitment
147 steps splitting reads among closely related genomes (Evans and Denef 2020). While the 95%
148 ANI cutoff is broadly recognized in contemporary microbiology as a threshold to identify
149 microbial species, it over-splits ecologically and evolutionarily cohesive units in SAR11 and
150 does not delineate species-like groups. We note that the reason behind our use of the 95% ANI in
151 this step of our analysis was solely to establish a technically robust workflow prior to
152 competitive read recruitment rather than a biologically meaningful partitioning of our genomes, a
153 challenge our study focuses on later.

154 We then turned our attention to the distal end of the phylogeny, which contained a large
155 number of well supported clusters of closely related genomes, particularly within the Ia/Ib
156 subgroup that contained 78 of the 81 new isolate genomes. A phylogeny of the resulting 268
157 genomes revealed 24 monophyletic clusters within the historical Ia/Ib subgroup that were
158 characterized by a range of gANI values from 84% to 96% ($92.1 \pm 2.94\%$; mean \pm SD) (Fig. 1,
159 Supplemental Fig. 3). While a handful of these clusters were recognized previously, we defined
160 an additional 11 here (Fig 1; Supplemental Table 5). Twelve of the 24 clusters contained an
161 isolated representative, and eight contained at least one isolate from our study area in the tropical
162 Pacific.

163 In summary, our extensive phylogenomic analysis of SAR11 revealed 24 monophyletic
164 clusters within the historical Ia/Ib subgroup which included the majority of SAR11 SAGs and the

165 new and previously published isolate genomes. The non-uniform minimum gANI estimates
166 suggest that the application of sequence-based ANI thresholds to demarcate SAR11 diversity
167 may obscure important evolutionary signals. Hypothesized drivers of the maintenance and
168 partitioning of genomic diversity in SAR11 include niche-based processes, where genetically
169 cohesive clusters also display ecological homogeneity and the underlying genetic diversity is
170 maintained by similar forces of selection, recombination, and drift. To understand the potential
171 eco-evolutionary forces that shape SAR11 diversification, we turned to metagenomic read
172 recruitment analysis to recover biogeographical distribution patterns for our genomes across the
173 globe.



174

175 **Fig 1. Comprehensive phylogenies of the *Pelagibacteriales*.** A comparison between an
 176 exhaustive phylogeny (left panel) with 481 SAR11 genomes (106 isolates and 375 SAGs) and a
 177 pruned phylogeny (right panel) with 268 genomes (50 isolates and 218 SAGs), based on a
 178 curated SAR11-specific set of 165 genes. Genomes included in the pruned phylogeny are
 179 indicated with a dark blue bar in the left panel, and the origin of isolate genomes is indicated for
 180 both phylogenies.

181

182 Global read recruitment from the surface ocean reveals broadly congruent phylogenetic

183 and ecotypic diversification across SAR11

184 Our competitive metagenomic read recruitment assessed the distribution of the 268

185 SAR11 genomes around the globe and relied upon 950 publicly-available marine metagenomes,

186 as well as metagenomes from the Kāne‘ohe Bay Time-series (KByT), the location of isolation

187 for the 81 new and 9 of the 25 existing isolate genomes (Supplemental Table 6; Supplemental

188 Table 7). These data enabled us to investigate whether cohesive genomic and ecological groups,

189 or ecotypes, could be discerned by combining SAR11 phylogeny and biogeography.

190 Our first priority was to establish whether genome clusters within a given SAR11 clade

191 showed cohesive read recruitment profiles across metagenomes, or, in other words, whether the

192 ecological patterns revealed by a single genome were similar to all genomes within the group to

193 which it belonged. Detection values for multiple genomes within a genome cluster showed a

194 high degree of cohesion (Fig. 2; Supplemental Table 8; Supplemental Table 9). For example,

195 representatives from Ia.3.IV, Ia.3.I, Ia.4_I, Ia.4.N2, Ia.4.N5, Ib.1.III, and Ib.4.N9 are particularly

196 consistent within the genome clusters (Fig. 2). Consistent overlap between SAGs and isolate

197 genomes within the same clade demonstrated that both genome types accurately reflect

198 distribution patterns for closely related populations as inferred by phylogeny (Fig. 2). A

199 non-metric multidimensional scaling (NMDS) analysis of the overall detection patterns of

200 genomes across metagenomes consistently grouped genomes within a given clade more closely

201 compared to those that belonged to other genome clusters (Supplemental Fig. 4), further

202 supporting a high degree of intra-clade ecological cohesion.

203 Our second priority was to establish insights into whether SAR11 genome clusters
204 differed in their biogeographical patterns, and whether genome clusters identified SAR11
205 populations of distinct ecology. Hierarchical clustering of metagenomes based on SAR11
206 detection patterns revealed four groups: metagenomes that originated from (1) low-latitude
207 samples, (2) high-latitude samples with low SAR11 diversity, (3) low-latitude samples with high
208 SAR11 diversity, as well as (4) samples from coastal Kāne‘ohe Bay (Fig. 2). Many SAR11
209 genome clusters were indeed differentially distributed across these metagenome groups. For
210 example, Ia.4.II and Ia.4.N5 were only consistently found in groups 3 and 4, while Ia.3.IV was
211 found across group 1 and only in select sites in groups 3 and 4 (Fig 2). However, in multiple
212 cases, the environmental detection patterns of different phylogenomic genome clusters
213 overlapped; while there was some degree of inter-clade ecological differentiation, distinct
214 SAR11 genome clusters frequently co-occurred (Fig. 2, Supplemental Fig. 5). This observation
215 suggests that patterns of distribution alone cannot discern the boundaries of cohesive ecological
216 units within SAR11, a task that evidently requires the integration of biogeographical patterns
217 through metagenomic read recruitment with ancestral relationships among genomes though
218 phylogenomics.

219 Finally, we used the read recruitment analysis to assign ecological patterns to specific
220 SAR11 genome clusters. While multiple broad patterns were clear from the pairing of the
221 phylogenomic relationships and read recruitment data, we focused our investigation on whether
222 the genome clusters within the SAR11 Ia/Ib lineage that appeared to be confined to the coastal
223 end of the KByT environmental gradient (Ia.3.VI, Ia.3.II, and Ia.3.III; Supplemental Fig. 1; also
224 see (Tucker et al. 2024a)) were similarly constrained to coastal areas globally. Indeed, two of the

225 three genome clusters, Ia.3.II and Ia.3.III, were detected almost exclusively in metagenomes
226 sourced from coastal environments (e.g., KByT, the north coast of Panama, the Chesapeake Bay,
227 and the Atlantic coast of Portugal). Interestingly, while the clade Ia.3.VI was restricted to
228 nearshore metagenomes across KByT, it was well-detected in both coastal and offshore
229 environments in other oceanic regions (Fig. 2). Genome clusters Ia.3.II and Ia.3.III did not
230 include any SAGs and were only composed of isolates from coastal Kāne‘ohe Bay. Yet, we could
231 detect them in other oceans, which confirms their global relevance as representatives of SAR11
232 populations adapted to coastal ecosystems.

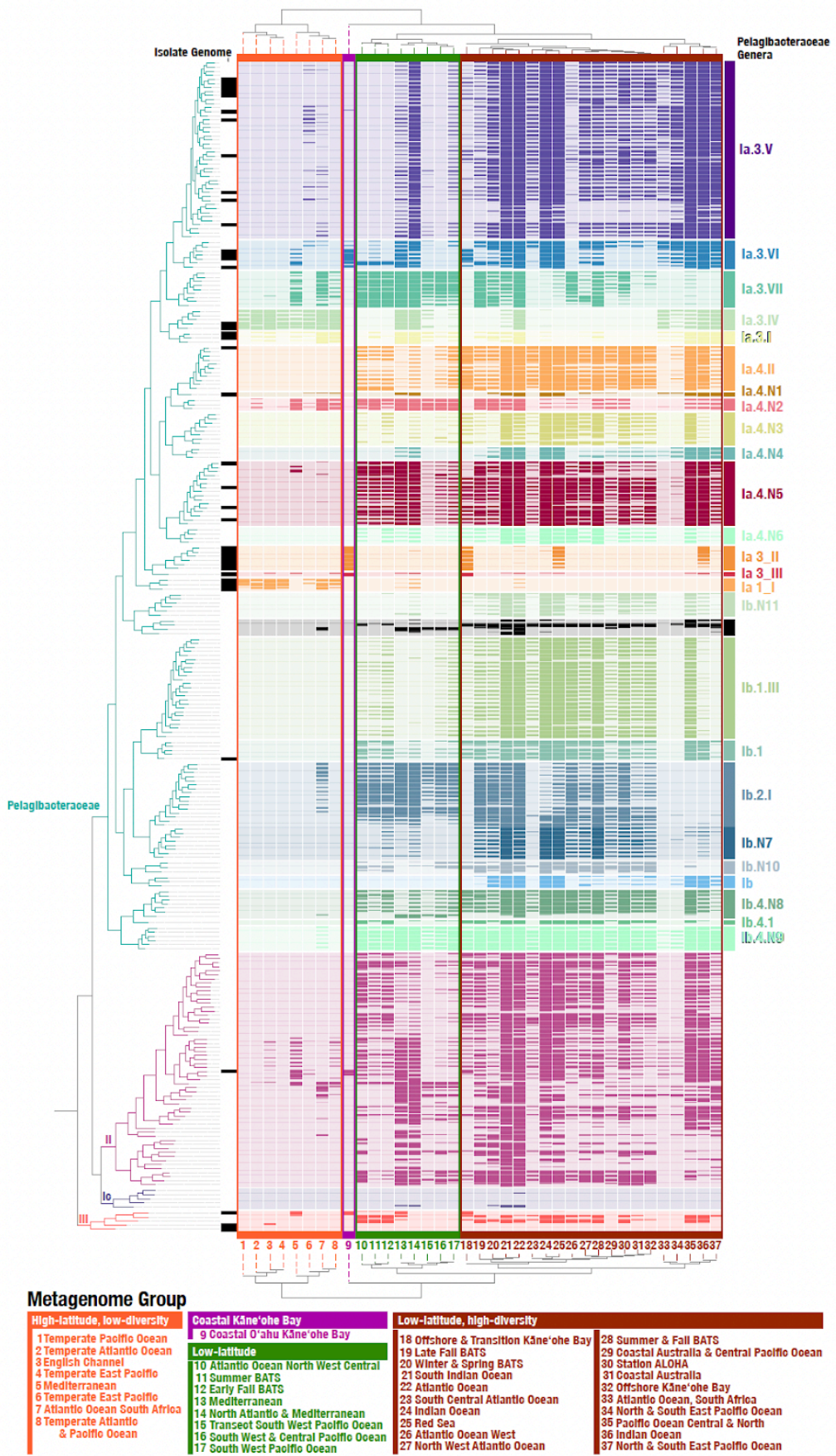
233 Through the combination of global metagenomic read recruitment and phylogenomics,
234 we show that SAR11 genome clusters contain genomes with a high degree of intra-clade
235 ecological cohesion. These genome clusters were often distinguished by their ecological
236 distributions and demonstrated notable inter-clade ecological differentiation. Finally, we applied
237 this framework to understand how SAR11 genetic and ecological diversity partitions among
238 ocean biomes, in particular coastal ocean and open ocean environments.

239 The integrated ecological and evolutionary framework here is supported by high-quality
240 genomes that span the known diversity of the *Pelagibacterales*, providing a critical opportunity
241 to discern distinct ecologically meaningful genome clusters within SAR11. We show that the 24
242 distinct genome clusters represent groups sharing cohesive ecological patterns and evolutionary
243 relationships, not at the finest tips of the phylogenomic tree, but at relatively deeper branches
244 that encompass gANI values ranging between 84% and 96%. This suggests it is unlikely that
245 these genome clusters represent SAR11 diversity at the level of ‘species’. This conclusion is
246 further supported by our companion work (Tucker et al. 2024a), which reveals systematic

247 differences in the metabolic potential of SAR11 genome clusters that likely support distinct
248 ecological distributions in immediately adjacent coastal and open ocean surface seawater with
249 habitat-specific metabolic genes that are under higher selective forces. With the combined
250 evidence presented here and in the work by Tucker et al. (2024a) that unite SAR11 diversity into
251 distinct genome clusters with ecotype properties supported by SAR11 phylogenomics, ecology,
252 metabolic potential, as well as population genetics, we argue that the most conceivable
253 taxonomic rank at which SAR11 genome clusters can be described in a conventional framework
254 emerges as the ‘genus’ level.

255 This genus-level designation is ideal as it encompasses a degree of diversity previously
256 designated by SAR11 subgroups and has the flexibility to account for subtle variation in ecology
257 recognized between closely related genomes. We identified the highest quality genome
258 representatives (electing for isolates when possible) to assign as type genomes for each genus
259 (Fig. 4), which establishes a roadmap to rationally designate new genera as they are identified in
260 the future.

261



263 **Fig. 2: Global metagenome read recruitment to 268 *Pelagibacterales* genomes.** A clustering
264 analysis reveals that the distribution of metagenomes from the same geographic location have
265 characteristic patterns of detection. Detection values from 0.25 to 0.75 are shown.

266

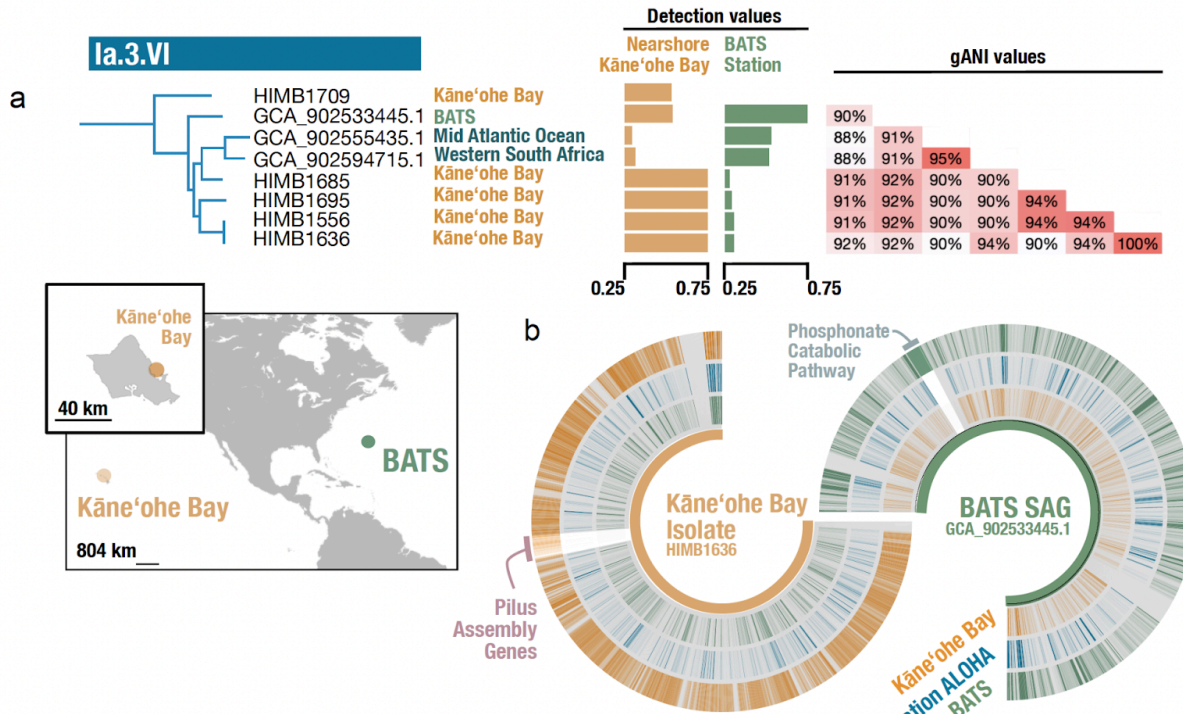
267 **Evidence for ecological speciation within closely related genome clusters**

268 Despite broad ecological cohesion within what we have designated as *Pelagibacterales*
269 genera, some notable differences highlight underlying complexities in defining the finest scales
270 of divergence. The Ia.3.VI genus includes genomes from strains of Kāne‘ohe Bay origin as well
271 as SAGs from other regions of the global ocean and encompasses significant genomic diversity
272 (minimum gANI 88%) and phylogenomic structure (Fig. 3a). Through read recruitment, we
273 observed notable differences in detection patterns of genomes across metagenomic samples.

274 Isolate genomes from the bay harbored the highest detection values of the Ia.3.VI genus from
275 metagenomes in the bay, while a SAG from the BATS site in the Atlantic Ocean
276 (GCA_902533445.1) had the highest detection values at the BATS site (Fig. 3a), particularly in
277 the summer and fall (Fig. 2).

278

279



280

281 **Fig. 3: Fine-scale ecological speciation between closely related SAR11 genomes. (a)** Detailed
 282 view of the Ia.3.VI genus including evolutionary relationships, locations of genome origin,
 283 detection values from select locations, and within-genus gANI values. The geographic origins of
 284 two of the closely related genomes that have distinct detection patterns include Kāne'ohe Bay in
 285 the Pacific Ocean and the Bermuda Atlantic Time-series Study (BATS) in the Atlantic. **(b)**
 286 Coverage values of isolate HIMB1636 and SAG GCA_902533445.1 of metagenomes from
 287 nearshore Kāne'ohe Bay, Station ALOHA in the North Pacific Subtropical Gyre, and BATS
 288 highlighting the differential detection of genes for type IV pilus assembly and the phosphonate
 289 catabolic pathway.

290

291 Given the underlying genomic diversification between isolate HIMB1636 and BATS
 292 SAG GCA_902533445.1 and their distinct biogeographical distributions that peak in each of
 293 their respective source locations, we next surveyed the genomes for potentially unique metabolic
 294 capabilities. By inspecting the coverage of isolate HIMB1636 and BATS SAG
 295 GCA_902533445.1 using metagenomes from Kāne'ohe Bay and the BATS site (Supplemental
 296 Table 10), we found one genomic region of SAG GCA_902533445.1 that had particularly high

297 coverage at BATS compared to the KByT samples and included 29 genes encoding the uptake
298 (*phnCDE*) and catabolism of phosphonates via the C-P lyase pathway (*phnGHIJKLM*) (Fig. 3d)
299 (Villarreal-Chiu et al. 2012). The *phnJ* phylogeny did not reflect the phylogenomic relationships
300 among genomes (Supplemental Fig. 6), and the entire pathway was located on a genomic island
301 similar to the marine bacterium HIMB59 (Molina-Pardines et al. 2023). The C-P lyase pathway
302 is known to be enriched in phosphate-depleted systems of the Atlantic Ocean (Sosa et al. 2019;
303 Acker et al. 2022), so the presence of the C-P lyase catabolic genes in a genome sourced from
304 BATS, but missing from a closely related genome sourced from more phosphate-replete
305 environments of Kāne‘ohe Bay in the Pacific, suggests these genes provide an advantage in
306 phosphate depleted systems and that the BATS SAG GCA_902533445.1 may be locally-adapted
307 to these environments.

308 While the HIMB1636 genome lacked the C-P lyase pathway, it contained a unique
309 genomic region with particularly high coverage that was not found in SAG GCA_902533445.1,
310 and encoded genes for type IV pilus assembly. The role of type IV pilus assemblies in SAR11 is
311 unclear (Zhao et al., 2017), although in other organisms it has been associated with an array of
312 functions including DNA uptake, twitching motility, and aggregation into microcolonies (Craig
313 and Li 2008). The presence of the type IV pilus assembly genes in the Ia.3.VI genome sourced
314 from the nitrogen-limited Pacific Ocean, but not in genomes from relatively more
315 nitrogen-replete waters of BATS, along with evidence that the *Pelagibacteraceae* can utilize
316 purine nucleosides and purine-derivatives for nitrogen (Braakman et al. 2024; Tucker et al.
317 2024a), suggests that the presence of a type IV pilus may be advantageous for DNA uptake in
318 nitrogen-poor environments and that HIMB1636 may be locally-adapted. Contrary to the

319 hypothesis that genera recombine at a rate sufficient to limit the ecotypic diversification of
320 closely related genomes (Zhao et al. 2024), our read mapping instead shows that the HIMB1636
321 and SAG GCA_902533445.1 genomes within cluster Ia.3.VI have sufficiently diverged at the
322 nucleotide level to reveal clear biogeographic divergence, and that they possess sets of genes that
323 reside in hypervariable genomic regions that are clearly associated with the differences in
324 abundance.

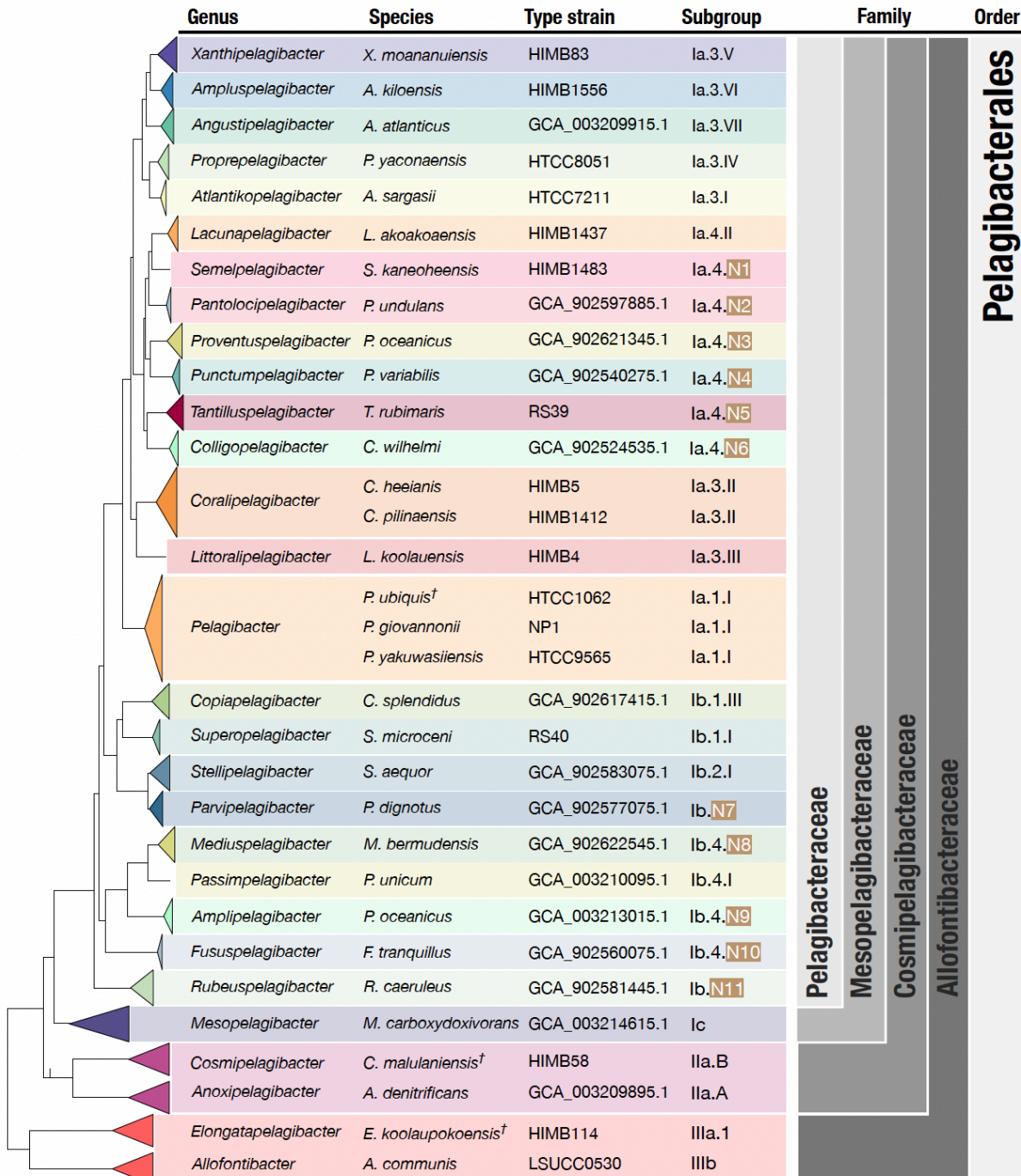
325 We examined gANI estimates, phylogenetic branching, environmental distributions, and
326 ecologically-relevant gene content to support the characterization of ecological diversification at
327 the finest tips of the tree, a process that we theorize to represent speciation. This underscores the
328 complexity of SAR11 ecology, highlights the need to include a diversity of representative
329 genomes within even closely related genera for environmental genomics studies, and indicates
330 that continued efforts to sample SAR11 globally are key to understanding the distribution of this
331 ubiquitous clade.

332

333 **Proposed *Pelagibacterales* classification and nomenclature**

334 We leveraged the robust genome phylogeny, gANI metrics, and read recruitment to
335 establish a rational classification and nomenclature system for the *Pelagibacterales* bacterial
336 order *Pelagibacterales*. To provide a framework and vocabulary to discuss groups of SAR11 in a
337 meaningful context, we first defined four family-level monophyletic groups as the
338 *Pelagibacteraceae* (historical subgroups Ia and Ib), *Cosmipelagibacteraceae* (historical
339 subgroup II), *Allofontibacteraceae* (historical subgroup III), and the *Mesopelagibacteraceae*
340 (historical subgroup Ic) (Fig. 4). We focused our efforts primarily on classification within the

341 *Pelagibacteraceae* where the majority of cultured isolates originate. Within the
342 *Pelagibacteraceae*, we used phylogenomics and ecological data to characterize 24 genera that
343 represent cohesive genetic and ecological clades, and designate type species for each
344 (Supplemental Table 11). The primary aim of these efforts is to ensure that the taxonomic
345 hierarchy for SAR11 provides a useful and tractable reflection of the ecology and genetic
346 diversity within this globally distributed group, and establishes a rational system that future
347 efforts can build upon.



348

349 **Figure 4. A proposed taxonomic framework for the SAR11 order *Pelagibacterales*.** This

350 schematic SAR11 phylogeny unites proposed genus and species names, proposed type strains,

351 and historical reference labels.

352 Discussion

353 By integrating high-throughput cultivation experiments with publicly available genomes
354 and metagenomes, our study provides key insights into a long-standing question: to what extent,
355 and at what hierarchical levels, can the genomic and ecological diversity of SAR11 be
356 partitioned into cohesive units? Through comprehensive phylogenomic analyses paired with
357 global metagenomic read recruitment surveys, we reveal ecotypic differentiation at both
358 relatively shallow, species-level and deeper, genus-level diversity within SAR11. This robust
359 eco-evolutionary framework, which unifies independent yet complementary approaches to
360 genomic diversity and biogeography, resolves the order *Pelagibacterales* into four families and
361 the family *Pelagibacteraceae* into 24 genera, establishing a much-needed taxonomic framework
362 that delineates SAR11 diversity into tractable units and provides a foundation for future
363 investigations.

364 A tight relationship between the phylogeny and ecology of SAR11 has long been
365 suggested (Brown et al. 2012; Vergin et al. 2013); however, the ability to associate specific
366 SAR11 clades with distinct ecological patterns and explain forces that maintain SAR11 diversity
367 has remained elusive. Focusing on sequence-discrete groups within deep ocean SAR11 lineages,
368 a recent study concluded that recombination, rather than ecological speciation, was likely the
369 major driver of species-level cohesion (Zhao et al., 2024). While this observation may explain
370 forces that maintain species-level cohesion for some populations in this group, our study shows
371 that the global sampling of environmental populations through metagenomes consistently
372 supports ecological delineations that are congruent with phylogenomic clustering patterns,

373 pointing towards ecotypic differentiation as the pervasive driver of the evolution within the
374 *Pelagibacterales*. Interestingly, SAR11 genera that showed similar biogeographical distribution
375 patterns in our analysis tended to occupy distant parts of the tree. This observation suggests an
376 inverse correlation between the genetic similarity among SAR11 populations and their
377 co-occurrence, a trend known as phylogenetic overdispersion. Phylogenetic overdispersion has
378 been observed across the tree of life (Davies 2006) and is driven by forces of competitive
379 exclusion, an overarching ecological phenomenon that limits the co-occurrence of ecologically
380 similar, closely related organisms. Future analyses that aim to resolve specific genetic
381 determinants of competitive exclusion or co-existence may benefit from geographically
382 constrained time-series data, as these patterns are likely not immediately attainable from global
383 yet spatiotemporally sparse metagenomes.

384 The practical need of microbiologists to find reasonable cutoffs to demarcate species
385 boundaries from genomic data alone and the nature of SAR11 evolution do not align seamlessly.
386 Through the analysis of genomes, a large number of anecdotal observations support 95% ANI as
387 a reasonable means to resolve archaeal and bacterial species (Jain et al. 2018; Olm et al. 2020).
388 However, SAR11 serves as a reminder that practical solutions do not necessarily apply to all
389 microbial clades (Delmont et al. 2019; López-Pérez et al. 2020). One of the implications of the
390 efforts to standardize the tree of life based on principles that work only for the majority of
391 microbial taxa is the conflation of all SAR11 genomes into two genera in the taxonomic
392 framework derived from genomes available on GTDB based on RED scores (Parks et al. 2022).
393 Indeed, while the ecologically relevant units of SAR11 described in our study are in agreement
394 with functional, evolutionary, and ecological observations, they are in disagreement with the

395 contemporary summaries of this clade based on RED- or ANI-based demarcations. The ways in
396 which evolutionary relationships between distinct clades of life intersect with taxonomic
397 classification systems will unlikely be resolved in a manner that satisfies everyone in
398 microbiology (Waite et al. 2020; Sanford et al. 2021). In this juncture, we believe that a stronger
399 motivation to understand the biological drivers that render SAR11 incompatible with our best
400 practical approaches will bring us closer to a unified solution to partition microbial diversity into
401 meaningful units, rather than casting SAR11, one of the most numerous microbial clades on our
402 planet, as a mere outlier.

403 Insights into the eco-evolutionary processes that shape SAR11 diversification in our
404 study rely heavily on the contribution of 81 new isolate genomes that represent abundant and
405 ecologically-relevant SAR11 populations across the coastal and global ocean. The
406 ecology-informed hierarchical organization of these genomes enabled us to propose SAR11
407 genera with formal names here, and investigate the likely functional determinants of ecological
408 diversification across the *Pelagibacteraceae* in our companion work (Tucker et al. 2024a). While
409 deeper understanding of the physiological, metabolic, and genetic factors that shape SAR11
410 biology will require controlled experimentation of isolated strains in the laboratory, our study
411 organizes the eco-evolutionary characteristics of known SAR11 diversity and provides a
412 roadmap for future efforts aimed to organize and understand the ubiquitous SAR11 populations
413 inhabiting the global ocean.

414

415 Methods

416 High-throughput culturing from surface seawater within and adjacent to Kāne‘ohe Bay,

417 O‘ahu

418 Growth medium was prepared as previously described (Monaghan et al., 2020). Briefly,
419 20 L of seawater was collected first on 8 July 2017 and again on 20 September 2017 from a
420 depth of 2 meters at station SR4 (N 21° 27.699', W 157° 47.010') in acid-washed polycarbonate
421 bottles (Supplemental Fig. 1). The seawater was then filtered, autoclaved, and sparged as
422 previously described (Monaghan et al. 2020). After processing, the sterile seawater was stored at
423 4°C until use.

424 Two 4 L seawater samples to be used as inoculum were collected on 26 July 2017 in
425 acid-washed polycarbonate bottles from 2 meters from stations SB (N 21° 26.181', W 157°
426 46.642) and STO1 (N 21° 28.974, W 157° 45.978') (Supplemental Fig. 1) and immediately
427 returned to the laboratory for further processing. All of the Kāne‘ohe Bay Time series sampling
428 sites were previously classified as ‘nearshore’, ‘transition’, or ‘offshore’, with SB and STO1
429 representing nearshore and offshore sites, respectively (Tucker et al. 2021). Subsamples of the
430 raw seawater were processed as described previously (Monaghan et al. 2020). Briefly, aliquots
431 were taken for cryopreservation in a final concentration of 10% v/v glycerol and fixed with
432 paraformaldehyde for the enumeration of planktonic microorganisms via flow cytometry.

433 Additionally, 0.96 L from station SB and 1.30 L from station STO1 were filtered through a 25
434 mm diameter, 0.1 µm pore-sized polyethersulfone membrane (Supor-100; Pall Gelman Inc., Ann

435 Arbor, MI), which was then submerged in 500 μ L DNA lysis buffer and stored at -80°C until

436 DNA extraction.

437 Subsamples of raw seawater from SB and STO1 were enumerated using microscopy,

438 diluted to 2.5 cells mL^{-1} , and plated in 2 mL volumes into a total of 1,152 wells (576 wells per

439 site) of custom-fabricated 96-well Teflon microtiter plates. This experiment is referred to here as

440 HTC2017. Plates were then sealed with breathable polypropylene microplate adhesive film and

441 incubated in the dark at 27°C. Plates were monitored for cellular growth at 3.5 and 8 weeks using

442 flow cytometry as previously described (Tripp et al. 2008; Monaghan et al. 2020). Wells with

443 positive growth (greater than 10^4 cells mL) after 24 or 57 days of incubation were further

444 sub-cultured by transferring approximately 1 mL into 20 mL of sterile seawater media amended

445 as previously described (Monaghan et al. 2020) with 400 μM $(\text{NH}_4)_2\text{SO}_4$, 400 μM NH_4Cl , 50 μM

446 NaH_2PO_4 , 1 μM glycine, 1 μM methionine, 50 μM pyruvate, 800 nM niacin (B3), 425 nM

447 pantothenic acid (B5), 500 nM pyridoxine (B6), 4 nM biotin (B7), 4 nM folic acid (B9), 6 μM

448 myo-inositol, 60 nM 4-aminobenzoic acid, and 6 μM thiamine hydrochloride (B1). These

449 subcultures were then incubated at 27°C in the dark for an additional 33 days and then all

450 samples were processed and cataloged.

451 Cultures checked at 33 days that yielded positive growth ($>10^4$ cells ml^{-1}) were

452 cryopreserved in duplicate (2 x 500 μL culture and a final concentration of 10% v/v glycerol).

453 Each well with positive growth was assigned an HIMB culture ID and cells from the

454 approximately 18 mL remaining volume of each culture were collected by filtration through a 13

455 mm diameter, 0.03 μm pore-sized polyethersulfone membrane (Sterlitech, Kent, WA, USA),

456 which was then submerged in 250 μL DNA lysis buffer and stored at -80°C until DNA

457 extraction. The lysis buffer was prepared by adding the following to MilliQ water: 8 mL 1M Tris
458 HCl (pH 8.0), 1.6 ml 0.5M EDTA (pH 8.0), and 4.8 g Triton X, for a final volume of 400 mL,
459 which was then filter sterilized, with lysozyme added to aliquots immediately before use (at a
460 final concentration of 20 mg ml⁻¹).

461 An additional experiment was performed using cryopreserved samples of seawater
462 collected on July 26, 2017, and described previously (Monaghan et al. 2020). Briefly, the
463 cryopreserved sample was enumerated and then diluted to two cell concentrations (2.5 and 52.5
464 cells ml⁻¹), and used to plate 480 and 470 2-ml dilution cultures, respectively. This experiment is
465 referred to as HTC2018. Growth was monitored at 2, 3, and 5 weeks after inoculation with
466 positive growth ($>10^4$ cells ml⁻¹) from the 2.5 cells ml⁻¹ cultures subcultured into 20 ml of sterile
467 seawater growth medium and monitored for growth for up to 10 weeks at 27°C in the dark.
468 Subcultures were then cryopreserved and cells collected for DNA sequencing as described
469 above. One well from the 52.5 cells ml⁻¹ inoculation was directly collected for DNA sequencing
470 without subculturing (Monaghan et al. 2020).

471 **DNA extraction and 16S rRNA gene amplicon sequencing**

472 Genomic DNA (gDNA) from all filtered cultures as well as environmental DNA (eDNA)
473 from STO1 and SB was extracted using the Qiagen DNeasy Blood and Tissue Kit with modified
474 manufacturer's instructions for bacterial cells (Qiagen, Germantown, Maryland, USA). The
475 modifications included the addition of an initial freeze-thaw step (3 cycles of 10 minutes at 65°C
476 followed by 10 minutes at -80°C), the addition of 35 µL Proteinase K and 278 µL buffer AL at
477 the appropriate pretreatment step, and finally when eluted the same 200 µL volume was passed
478 through the membrane three times.

479 For the initial identification of all cultures, gDNA was used as template for the
480 polymerase chain reaction (PCR) amplification (Bio Rad C1000 Touch, Bio Rad, Hercules, CA,
481 USA) using barcoded 515F and 926R primers targeting the V4 region of the SSU rRNA gene
482 (Parada et al., 2016) in a reaction volume of 25 µL composed of: 2 µL gDNA, 0.5 µL each
483 forward and reverse primer, 10 µL 5PRIME HotMasterMix (Quantabio, Beverly, MA, USA),
484 and 12 µL of molecular grade H₂O (Monaghan et al. 2020). The reaction was as follows: an
485 initial denaturation step of 3 min at 94°C, 40 cycles of 45 sec at 94°C followed by 1 min at 50°C
486 and 1.5 min at 72°C, with a final extension of 10 min at 72°C. The PCR products were prepared
487 for sequencing as previously described (Monaghan et al. 2020) and sequenced on a MiSeq
488 platform by the Oregon State University Center for Genome Research and Biocomputing.

489 **16S rRNA gene sequence analysis**

490 Amplicon sequence data were processed as previously described (Monaghan et al. 2020).
491 Briefly, the data was imported into QIIME2 v2019.4.0, and demultiplexed before being assessed
492 for sequence quality and merged. DADA2 (Callahan et al. 2016) was then used for quality
493 control. Taxonomy was assigned to all reads using a Naïve Bayes classifier trained on the Silva
494 rRNA v132 database (Quast et al. 2013). Cultures were first classified as defined previously
495 (Monaghan et al. 2020), with “monocultures” consisting of more than 90% of reads from a single
496 amplicon sequence variant (ASV), “mixed cultures” with an ASV that was between 50% and
497 90% of the reads, and finally cultures with no dominant members. Any samples with less than
498 1,000 reads were not included in further analyses. We aimed to sequence all strains that included
499 monocultures and mixed cultures of SAR11.

500 Genome sequencing

501 To prepare samples of interest for whole genome sequencing, all extractions with gDNA
502 concentrations above $0.06 \text{ ng } \mu\text{L}^{-1}$, a total of $10 \mu\text{L}$ were aliquoted for sequencing. For samples
503 with concentrations below $0.06 \text{ ng } \mu\text{L}^{-1}$, the remaining extraction volume (approximately 175 to
504 $185 \mu\text{L}$) was concentrated using a SpeedVac (ThermoFisher) to approximately $30 \mu\text{l}$ and was
505 re-quantified (Qubit 2.0, Invitrogen). From the concentrated samples with a minimum of 0.06 ng
506 μL^{-1} , $10 \mu\text{L}$ was aliquoted for sequencing. Samples for sequencing were prepared using a
507 Nextera library kit and sequenced on the NextSeq500 platform via a 150 bp paired-end run.

508 Genomes for previously cultured strains HIMB109 and HIMB123 (Brandon 2006) were
509 sequenced by the Joint Genome Institute. Multiple methods were used to sequence these two
510 strains, including directly using $200 \mu\text{L}$ of cell culture for library prep as well as using multiple
511 volumes (5, 10, or $20 \mu\text{L}$) of culture for multiple displacement analysis (MDA) prior to library
512 preparation. The genomes were evaluated based on completeness, length, number of reads, and
513 total contigs post assembly using SPAdes (Bankevich et al. 2012). An additional assembly using
514 all reads generated from various sequencing attempts per genome was also constructed using the
515 same assembly method, the highest quality genomes based on the metrics above were manually
516 curated and used for additional analyses.

517 Genome assembly and assessment

518 Short reads were trimmed with Trim Galore!
519 (<https://github.com/FelixKrueger/TrimGalore>) and assembled using Unicycler (Wick et al. 2017),
520 which acts as a SPAdes (Bankevich et al. 2012) optimizer with Illumina short read data. Once
521 assembled, reference indexes were built, and read mapping was performed using Bowtie2 with

522 default parameters (Langmead and Salzberg 2012). SAMtools (Li et al. 2009) was used to
523 convert the SAM file to a sorted and indexed BAM file. These initial assemblies and BAM files
524 were used to visualize genomes in anvi'o to check for possible contamination (Eren et al. 2015,
525 2021). For genomes with contamination, (determined visually as instances where contigs had
526 anomalous GC content or tetranucleotide frequency), suspicious contigs were removed.
527 Redundancy was also used as a way to flag any genomes that needed further curation. After
528 inspection, curated contigs were exported using the program 'anvi-summarize' and reads were
529 re-mapped to the cleaned version of assemblies. The cleaned genomes were processed again for
530 visualization in anvi'o to ensure no erroneous contigs were included. Mapping quality was
531 inspected visually using the Integrative Genomics Viewer (IGV) (Robinson et al. 2011) and
532 Tablet (Milne et al. 2013) and manual curation was undertaken using mapped read data. Manual
533 inspection was used to determine if a circular genome could be considered closed and complete.
534 All contigs shorter than 1000 bp were removed from the genomes that were not closed after final
535 curation, and anvi'o was used to assess final genome completeness and redundancy (Eren et al.
536 2021).

537 Phylogenomic analyses

538 To generate a comprehensive phylogeny of the SAR11 clade, a suite of high-quality
539 genomes were curated. Even with an abundance of metagenomes, the high diversity among
540 SAR11 populations makes constructing reliable MAGs currently unfeasible, so to ensure the
541 phylogeny was as robust as possible, only isolate genomes and SAGs were included. The final
542 set of 493 SAR11 genomes for phylogenetic reconstruction included 81 genomes sequenced in
543 this study, 25 previously published reference genomes, and 387 previously published single

544 amplified genomes (SAGs), in addition to 20 isolate genomes from the family Rhodobacteraceae
545 that were used as an outgroup (Supplemental Table 3). The majority of SAGs included were
546 equal to or greater than 85% complete according to checkM (Parks et al. 2015). However,
547 genomes of lower quality from subclades of SAR11 with no high-quality representatives were
548 included to produce a comprehensive phylogeny, for example SAR11 Ic genomes that ranged
549 from 56.0 to 93.7 percent completion were also included (Thrash et al. 2014) (Supplemental
550 Table 3). Both previously identified subgroup V and IV genomes were excluded from these
551 analyses as subgroup V is not considered to be within SAR11 and the inclusion of subgroup IV
552 has not been rigorously investigated and thus its relationship to the *Pelagibacterales* is
553 questionable (Thrash et al. 2011; Viklund et al. 2013; Haro-Moreno et al. 2020; Muñoz-Gómez
554 et al. 2022).

555 We compared two gene sets to determine the most appropriate genes to use for
556 phylogenetic reconstructions of the SAR11 clade. This included the bac120 gene set utilized by
557 GTDB-Tk to determine the bacteria guide tree, and a curated gene set of marker genes derived
558 from the 200-genes previously demonstrated to be best fit for the *Alphaproteobacteria*
559 (Muñoz-Gómez et al. 2019) (Supplemental Table 4). To curate the second gene set, we generated
560 a custom HMM profile for the 200 *Alphaproteobacteria* genes with a noise cutoff term of
561 1×10^{-20} , ran the HMM profile on all genomes using the anvi'o program 'anvi-run-hmms', and
562 generated a presence-absence matrix of genes in this model across genomes using the program
563 'anvi-script-gen-hmm-hits-matrix-across-genomes'. After evaluating the model hits across the
564 genomes matrix, we removed the genes that occurred in less than 90% of the genomes or those
565 that were redundant in more than 2% of the genomes from the *Alphaproteobacteria* 200-gene

566 collection, which resulted in a new collection with 165 genes, which is referred to as the
567 `SAR11_165` throughout our study (Supplemental Table 4). To generate a concatenated
568 alignment of the genes of interest for downstream phylogenomic analyses, a custom HMM
569 source was generated that encompassed the SAR11_165 genes. The program
570 `anvi-get-sequences-for-hmm-hits` with the custom HMM source was then implemented to
571 extract and align genes of interest. The program trimAL 1.3 (Capella-Gutiérrez et al. 2009) was
572 then used to remove all positions that were missing in more than 50% of the genomes.
573 Phylogenies were generated with IQ-Tree v2.1.2 (Minh et al. 2020) with the best fit model
574 (LG+F+R10) chosen using ModelFinder (Kalyaanamoorthy et al. 2017) and 1,000 ultrafast
575 bootstraps. Phylogenies were rerooted appropriately in FigTree, and exported in NEXUS format
576 with the options selected to “Save as currently displayed” and “Include Annotations (NEXUS &
577 JSON only)”. Once exported, phylogenies were then compared using the package phytools
578 (Revell 2024) in R (R Development Core Team 2011).

579 Once the extended phylogeny was established, a subset of SAR11 genomes was used to
580 generate a pruned phylogeny with the SAR_165 gene set. For this, we first used PyANI
581 (Pritchard et al. 2016) to derePLICATE all genomes using 95% gANI as a cutoff, then excluded
582 SAGs that did not share at least 90% gANI with a neighboring genome, and finally included 10
583 genomes from the GTDB that spanned 10 families from the order *Rhodospirillales* as an
584 outgroup prior to recomputing the final phylogenomic tree as described above. The 95% ANI
585 derePLICATION cutoff was chosen to avoid read splitting during competitive read recruitment and
586 for any clusters in which isolate genomes were available, they were chosen as preferred
587 representatives.

588

589 Classification and nomenclature

590 The extended phylogeny was used to define cohesive genetic clusters at the distal end of
591 the SAR11 tree. Single genomes that did not share at least 90% ANI with a neighboring genome
592 were not classified into genera.

593 To determine how taxonomic levels across the SAR11 lineage would compare using
594 relative evolutionary distance, we implemented this approach as previously described (Ramfelt et
595 al. 2024). Briefly, a domain-level phylogeny was first constructed using the GTDB-Tk
596 de_novo_workflow (Chaumeil et al. 2019) with SAR11 isolate and SAGs as well as
597 "p_Chloroflexota" as the outgroup. Marker genes were identified from the input genomes using
598 GTDB-Tk 'identify', and then aligned with GTDB-Tk 'align' (using the "--skip_gtdb_refs"
599 flag). Finally, a tree was constructed using FastTree v2.1.10 (model WAG+GAMMA) (Price et
600 al. 2010), rooted with the Chloroflexota outgroup. This phylogeny was used as the input for the
601 'scale_tree' program in PhyloRank v0.1.11 (<https://github.com/dparks1134/PhyloRank>) to
602 convert branch lengths into relative evolutionary distance (RED). RED values of 0.77 and 0.92
603 were used to assess how they would align with family and genus-level lineages, respectively.
604 These values were based on the distribution of internal nodes within the SAR11 clade and values
605 used previously for other family and genus-level lineages (Parks et al. 2018).

606

607 Read recruitment

608 To assess the distribution of the newly described strains described in this study and put
609 them into context with previously sequenced genomes, we used a read recruitment approach with

610 globally distributed metagenomes. The SAR11 genomes included in this study were grouped into
611 clusters that shared 95% average nucleotide identity (ANI) or greater and representatives from
612 these 95% gANI groups were then used for read recruitment (n = 314, Supplemental Table 12).
613 Results from read recruitment were extrapolated for the other genomes included in each 95%
614 gANI group.

615 Metagenomes used for recruitment included those sequenced in Kāne‘ohe Bay (Tucker et
616 al. 2024b), the environment from which the genomes were isolated. Only samples from sites
617 previously categorized as “nearshore” and “offshore” (Tucker et al. 2024b) were used here.
618 Additionally, globally distributed previously published metagenomes were also used including
619 those from TARA Oceans expeditions (Sunagawa et al. 2015), station ALOHA (Mende et al.
620 2017), GEOTRACERS cruises (Biller et al. 2018), the eastern coast of Japan (Kudo et al. 2018;
621 Yoshitake et al. 2021), Monterey Bay (Mueller et al. 2015), and the ocean sampling day program
622 (Kopf et al. 2015) (Supplemental Table 6 for a list of appropriate references and details regarding
623 metagenomes included).

624 Once metagenomes were chosen, raw reads were downloaded using 'prefetch' and
625 'fasterq-dump' in the SRA toolkit. We automated the quality filtering of metagenomes,
626 metagenomic read recruitment, and profiling of recruited reads using the program
627 anvi-run-workflow (Shaiber et al. 2020) with the '--workflow metagenomics' flag, which
628 implements snakemake (Köster and Rahmann 2012) recipes for standard analyses in anvi'o.
629 Briefly, this workflow identified and discarded the noisy sequencing reads in metagenomes using
630 the program 'iu-filter-quality-minoche' (Eren et al. 2013b), used SAR11 genomes to
631 competitively recruit short reads from metagenomes using Bowtie2 (Langmead and Salzberg

632 2012) SAMtools (Li et al. 2009) using the program `anvi-profile` , and finally merge individual
633 profiles into an anvi'o merged profile database using the program `anvi-merge` . The resulting
634 anvi'o merged profile database included essential data, including genome coverages and
635 detection statistics across metagenomes, for our downstream analyses. For coverage, we
636 primarily used the ‘mean coverage Q2Q3’ statistic, which represents the interquartile average of
637 coverage values where, for any given genome, the lowest 25% and the highest 25% of individual
638 coverage values are trimmed prior to calculating the average coverage from the remaining data
639 points, and thus minimizing the impact of biases due to highly conserved or highly variable
640 regions in the final coverage estimates. Visualization of read recruitment data mapped according
641 to the phylogeny constructed was completed using the program `anvi-interactive` with the
642 `--manual` flag.

643

644 Metagenome profile clustering

645 We performed a cluster analysis of metagenomes based on genome detection values from
646 the read recruitment step using the k-means algorithm, where we determined the `k` by
647 identifying the elbow of the curve of within-cluster sum of square values for increasing values of
648 `k` using the R code shared by Delmont et al. (2019) at <https://merenlab.org/data/sar11-saavs/>.
649 The results of the clustering analysis were visualized using anvi'o. To investigate how similar
650 detection patterns of genomes within genome clusters were, in addition to how similar or distinct
651 patterns were between genome-clusters, we performed a non-metric multidimensional scaling
652 (NMDS) analysis using the vegan package in R. Any metagenomes with zero detection across all

653 genomes were removed. The NMDS results were visualized using ggplot2 and plotly and an
654 interactive plot was generated with ggplotly.

655

656 Investigation of C-P lyase pathway

657 All genomes included in the extended phylogeny (n=X) were searched using
658 `anvi-search-functions` for the key enzyme in the C-P lyase pathway (*phnJ*) to determine the
659 capacity among high-quality SAR11 genomes to utilize the pathway. The genes upstream and
660 downstream of this essential gene were extracted from all 57 genomes and a pangenome was
661 used to compare the presence and absence of other key genes in the pathway as well as the
662 synteny of this region of the genome. The *phnJ* phylogeny (Supplemental Fig. 6) does not reflect
663 the relationships among genomes as demonstrated by the SAR_165 phylogeny (Fig. 1), which is
664 further evidence that this gene is located on a genomic island as previously described
665 (Molina-Pardines et al. 2023).

666 Acknowledgments

667 We thank Aimee Saito and Kerri Lettrell for their generous help with taxonomic names, Rex
668 Malmstrom and Nandita Nath for sequencing the genomes of isolates HIMB109 and HIMB123,
669 SeqCoast (formerly the Microbial Genome Sequencing Center) for sequencing isolate genomes,
670 Rachel Ouye for her help with HTC experiments, and Oscar Ramfelt for informatic support. This
671 research was supported by funding from the National Science Foundation to MSR
672 (OCE-1538628 and OCE-2149128). This is SOEST contribution xxx and HIMB contribution
673 xxx.

674 Competing interests

675 The authors declare no competing interests.

676 Data availability

677 The assembled sequence data for genomes reported here are available at FigShare at

678 <https://doi.org/10.6084/m9.figshare.28087454.v1>.

679 References

680 Acker, M., S. L. Hogle, P. M. Berube, T. Hackl, A. Coe, R. Stepanauskas, S. W. Chisholm, and D. J. Repeta. 2022. Phosphonate production by marine microbes: Exploring new sources and potential function. *Proc. Natl. Acad. Sci. U. S. A.* **119**: e2113386119.

683 Bankevich, A. and others. 2012. SPAdes: a new genome assembly algorithm and its applications to single-cell sequencing. *J. Comput. Biol.* **19**: 455–477.

685 Becker, J. W., S. L. Hogle, K. Rosendo, and S. W. Chisholm. 2019. Co-culture and biogeography of Prochlorococcus and SAR11. *ISME J.* **13**: 1506–1519.

687 Biller, S. J. and others. 2018. Marine microbial metagenomes sampled across space and time. *Sci Data* **5**: 180176.

689 Braakman, R. and others. 2024. Global niche partitioning of purine and pyrimidine cross-feeding among 690 ocean microbes. *bioRxiv*. doi:10.1101/2024.02.09.579562

691 Brandon, M. L. 2006. High-throughput isolation of pelagic marine macteria from the coastal subtropical

692 Pacific Ocean. University of Hawai‘i at Mānoa.

693 Brown, M. V. and others. 2012. Global biogeography of SAR11 marine bacteria. *Mol. Syst. Biol.* **8**: 595.

694 Callahan, B. J., P. J. McMurdie, M. J. Rosen, A. W. Han, A. J. A. Johnson, and S. P. Holmes. 2016.

695 DADA2: High-resolution sample inference from Illumina amplicon data. *Nat. Methods* **13**: 581–583.

696 Capella-Gutiérrez, S., J. M. Silla-Martínez, and T. Gabaldón. 2009. trimAl: a tool for automated

697 alignment trimming in large-scale phylogenetic analyses. *Bioinformatics* **25**: 1972–1973.

698 Carini, P., L. Steindler, S. Beszteri, and S. J. Giovannoni. 2013. Nutrient requirements for growth of the

699 extreme oligotroph “*Candidatus Pelagibacter ubique*” HTCC1062 on a defined medium. *ISME J.* **7**:

700 592–602.

701 Carlson, C. A., R. Morris, R. Parsons, A. H. Treusch, S. J. Giovannoni, and K. Vergin. 2009. Seasonal

702 dynamics of SAR11 populations in the euphotic and mesopelagic zones of the northwestern Sargasso

703 Sea. *ISME J.* **3**: 283–295.

704 Chang, T., G. S. Gavelis, J. M. Brown, and R. Stepanauskas. 2024. Genomic representativeness and

705 chimerism in large collections of SAGs and MAGs of marine prokaryoplankton. *Microbiome* **12**:

706 126.

707 Chaumeil, P.-A., A. J. Mussig, P. Hugenholtz, and D. H. Parks. 2019. GTDB-Tk: a toolkit to classify

708 genomes with the Genome Taxonomy Database. *Bioinformatics* **36**: 1925–1927.

709 Craig, L., and J. Li. 2008. Type IV pili: paradoxes in form and function. *Curr. Opin. Struct. Biol.* **18**:

710 267–277.

711 Davies, T. J. 2006. Evolutionary ecology: when relatives cannot live together. *Curr. Biol.* **16**: R645–7.

712 Delmont, T. O. and others. 2018. Nitrogen-fixing populations of Planctomycetes and Proteobacteria are

713 abundant in surface ocean metagenomes. *Nat Microbiol* **3**: 804–813.

714 Delmont, T. O., E. Kiefl, O. Kilinc, O. C. Esen, I. Uysal, M. S. Rappé, S. Giovannoni, and A. M. Eren.

715 2019. Single-amino acid variants reveal evolutionary processes that shape the biogeography of a

716 global SAR11 subclade. *Elife* **8**. doi:10.7554/eLife.46497

717 Eiler, A., D. H. Hayakawa, M. J. Church, D. M. Karl, and M. S. Rappé. 2009. Dynamics of the SAR11
718 bacterioplankton lineage in relation to environmental conditions in the oligotrophic North Pacific
719 subtropical gyre. *Environ. Microbiol.* **11**: 2291–2300.

720 Eren, A. M. and others. 2021. Community-led, integrated, reproducible multi-omics with anvi'o. *Nat
721 Microbiol* **6**: 3–6.

722 Eren, A. M., Ö. C. Esen, C. Quince, J. H. Vineis, H. G. Morrison, M. L. Sogin, and T. O. Delmont. 2015.

723 Anvi'o: an advanced analysis and visualization platform for 'omics data. *PeerJ* **3**: e1319.

724 Eren, A. M., L. Maignien, W. J. Sul, L. G. Murphy, S. L. Grim, H. G. Morrison, and M. L. Sogin. 2013a.

725 Oligotyping: Differentiating between closely related microbial taxa using 16S rRNA gene data.
726 *Methods Ecol. Evol.* **4**: 1111–1119.

727 Eren, A. M., J. H. Vineis, H. G. Morrison, and M. L. Sogin. 2013b. A filtering method to generate high
728 quality short reads using illumina paired-end technology. *PLoS One* **8**: e66643.

729 Evans, J. T., and V. J. Denef. 2020. To derePLICATE or not to derePLICATE? *mSphere* **5**.

730 doi:10.1128/mSphere.00971-19

731 Giovannoni, S. J. and others. 2005. Genome streamlining in a cosmopolitan oceanic bacterium. *Science
732* **309**: 1242–1245.

733 Giovannoni, S. J. 2017. SAR11 Bacteria: The Most Abundant Plankton in the Oceans. *Ann. Rev. Mar.
734 Sci.* **9**: 231–255.

735 Giovannoni, S. J., T. B. Britschgi, C. L. Moyer, and K. G. Field. 1990. Genetic diversity in Sargasso Sea
736 bacterioplankton. *Nature* **345**: 60–63.

737 Giovannoni, S. J., J. Cameron Thrash, and B. Temperton. 2014. Implications of streamlining theory for
738 microbial ecology. *ISME J.* **8**: 1553–1565.

739 Grote, J., J. C. Thrash, M. J. Huggett, Z. C. Landry, P. Carini, S. J. Giovannoni, and M. S. Rappé. 2012.

740 Streamlining and core genome conservation among highly divergent members of the SAR11 clade.

741 MBio **3**. doi:10.1128/mBio.00252-12

742 Haro-Moreno, J. M. and others. 2020. Ecogenomics of the SAR11 clade. Environ. Microbiol. **22**:

743 1748–1763.

744 Hug, L. A. and others. 2016. A new view of the tree of life. Nat Microbiol **1**: 16048.

745 Jain, C., L. M. Rodriguez-R, A. M. Phillippe, K. T. Konstantinidis, and S. Aluru. 2018. High throughput

746 ANI analysis of 90K prokaryotic genomes reveals clear species boundaries. Nat. Commun. **9**: 5114.

747 Kalyaanamoorthy, S., B. Q. Minh, T. K. F. Wong, A. von Haeseler, and L. S. Jermiin. 2017. ModelFinder:

748 fast model selection for accurate phylogenetic estimates. Nat. Methods **14**: 587–589.

749 Kiefl, E., O. C. Esen, S. E. Miller, K. L. Kroll, A. D. Willis, M. S. Rappé, T. Pan, and A. M. Eren. 2023.

750 Structure-informed microbial population genetics elucidate selective pressures that shape protein

751 evolution. Sci Adv **9**: eabq4632.

752 Kopf, A. and others. 2015. The ocean sampling day consortium. Gigascience **4**: 27.

753 Köster, J., and S. Rahmann. 2012. Building and documenting workflows with python-based Snakemake.

754 GCB **49**–56.

755 Kudo, T. and others. 2018. Seasonal changes in the abundance of bacterial genes related to

756 dimethylsulfoniopropionate catabolism in seawater from Ofunato Bay revealed by metagenomic

757 analysis. Gene **665**: 174–184.

758 Langmead, B., and S. L. Salzberg. 2012. Fast gapped-read alignment with Bowtie 2. Nat. Methods **9**:

759 357–359.

760 Li, H. and others. 2009. The Sequence Alignment/Map format and SAMtools. Bioinformatics **25**:

761 2078–2079.

762 López-Pérez, M., J. M. Haro-Moreno, F. H. Coutinho, M. Martinez-Garcia, and F. Rodriguez-Valera.

763 2020. The evolutionary success of the marine bacterium SAR11 analyzed through a metagenomic

764 perspective. *mSystems* **5**. doi:10.1128/mSystems.00605-20

765 Mende, D. R., J. A. Bryant, F. O. Aylward, J. M. Eppley, T. Nielsen, D. M. Karl, and E. F. DeLong. 2017.

766 Environmental drivers of a microbial genomic transition zone in the ocean's interior. *Nat Microbiol*

767 **2**: 1367–1373.

768 Milne, I., G. Stephen, M. Bayer, P. J. A. Cock, L. Pritchard, L. Cardle, P. D. Shaw, and D. Marshall. 2013.

769 Using Tablet for visual exploration of second-generation sequencing data. *Brief. Bioinform.* **14**:

770 193–202.

771 Minh, B. Q., H. A. Schmidt, O. Chernomor, D. Schrempf, M. D. Woodhams, A. von Haeseler, and R.

772 Lanfear. 2020. IQ-TREE 2: New Models and Efficient Methods for Phylogenetic Inference in the

773 Genomic Era. *Mol. Biol. Evol.* **37**: 1530–1534.

774 Molina-Pardines, C., J. M. Haro-Moreno, and M. López-Pérez. 2023. Phosphate-related genomic islands

775 as drivers of environmental adaptation in the streamlined marine alphaproteobacterial HIMB59.

776 *mSystems* **8**: e0089823.

777 Monaghan, E. A., K. C. Freel, and M. S. Rappé. 2020. Isolation of SAR11 Marine Bacteria from

778 Cryopreserved Seawater. *mSystems* **5**. doi:10.1128/mSystems.00954-20

779 Morris, R. M., M. S. Rappé, S. A. Connon, K. L. Vergin, W. A. Siebold, C. A. Carlson, and S. J.

780 Giovannoni. 2002. SAR11 clade dominates ocean surface bacterioplankton communities. *Nature*

781 **420**: 806–810.

782 Morris, R. M., K. L. Vergin, J.-C. Cho, M. S. Rappé, C. A. Carlson, and S. J. Giovannoni. 2005. Temporal

783 and spatial response of bacterioplankton lineages to annual convective overturn at the Bermuda

784 Atlantic Time-series Study site. *Limnol. Oceanogr.* **50**: 1687–1696.

785 Mueller, R. S. and others. 2015. Metagenome sequencing of a coastal marine microbial community from

786 monterey bay, california. *Genome Announc.* **3**. doi:10.1128/genomeA.00341-15

787 Muñoz-Gómez, S. A., S. Hess, G. Burger, B. F. Lang, E. Susko, C. H. Slamovits, and A. J. Roger. 2019.

788 An updated phylogeny of the Alphaproteobacteria reveals that the parasitic Rickettsiales and
789 Holosporales have independent origins. *Elife* **8**. doi:10.7554/eLife.42535

790 Muñoz-Gómez, S. A., E. Susko, K. Williamson, L. Eme, C. H. Slamovits, D. Moreira, P. López-García,
791 and A. J. Roger. 2022. Site-and-branch-heterogeneous analyses of an expanded dataset favour
792 mitochondria as sister to known Alphaproteobacteria. *Nat. Ecol. Evol.* **6**: 253–262.

793 Olm, M. R., A. Crits-Christoph, S. Diamond, A. Lavy, P. B. Matheus Carnevali, and J. F. Banfield. 2020.
794 Consistent metagenome-derived metrics verify and delineate bacterial species boundaries. *mSystems*
795 **5**. doi:10.1128/mSystems.00731-19

796 Pachiadaki, M. G. and others. 2019. Charting the complexity of the marine microbiome through
797 single-cell genomics. *Cell* **179**: 1623–1635.e11.

798 Paoli, L. and others. 2022. Biosynthetic potential of the global ocean microbiome. *Nature* **607**: 111–118.

799 Parks, D. H., M. Chuvochina, C. Rinke, A. J. Mussig, P.-A. Chaumeil, and P. Hugenholtz. 2022. GTDB:
800 an ongoing census of bacterial and archaeal diversity through a phylogenetically consistent, rank
801 normalized and complete genome-based taxonomy. *Nucleic Acids Res.* **50**: D785–D794.

802 Parks, D. H., M. Chuvochina, D. W. Waite, C. Rinke, A. Skarszewski, P.-A. Chaumeil, and P. Hugenholtz.
803 2018. A standardized bacterial taxonomy based on genome phylogeny substantially revises the tree
804 of life. *Nat. Biotechnol.* **36**: 996–1004.

805 Parks, D. H., M. Imelfort, C. T. Skennerton, P. Hugenholtz, and G. W. Tyson. 2015. CheckM: assessing
806 the quality of microbial genomes recovered from isolates, single cells, and metagenomes. *Genome*
807 *Res.* **25**: 1043–1055.

808 Price, M. N., P. S. Dehal, and A. P. Arkin. 2010. FastTree 2 – Approximately Maximum-Likelihood Trees
809 for Large Alignments. *PLoS One* **5**: e9490.

810 Pritchard, L., R. H. Glover, S. Humphris, J. G. Elphinstone, and I. K. Toth. 2016. Genomics and
811 taxonomy in diagnostics for food security: soft-rotting enterobacterial plant pathogens. *Anal.*

812 Methods **8**: 12–24.

813 Quast, C., E. Pruesse, P. Yilmaz, J. Gerken, T. Schweer, P. Yarza, J. Peplies, and F. O. Glöckner. 2013.

814 The SILVA ribosomal RNA gene database project: improved data processing and web-based tools.

815 Nucleic Acids Res. **41**: D590–6.

816 Ramfelt, O., K. C. Freel, S. J. Tucker, O. D. Nigro, and M. S. Rappé. 2024. Isolate-anchored comparisons

817 reveal evolutionary and functional differentiation across SAR86 marine bacteria. ISME J. **18**.

818 doi:10.1093/ismej/wrae227

819 Rappé, M. S., S. A. Connan, K. L. Vergin, and S. J. Giovannoni. 2002. Cultivation of the ubiquitous

820 SAR11 marine bacterioplankton clade. Nature **418**: 630–633.

821 R Development Core Team, R. 2011. R: A Language and Environment for Statistical Computing.,

822 Revell, L. J. 2024. phytools 2.0: an updated R ecosystem for phylogenetic comparative methods (and

823 other things). PeerJ **12**: e16505.

824 Robinson, J. T., H. Thorvaldsdóttir, W. Winckler, M. Guttman, E. S. Lander, G. Getz, and J. P. Mesirov.

825 2011. Integrative genomics viewer. Nat. Biotechnol. **29**: 24–26.

826 Sanford, R. A., K. G. Lloyd, K. T. Konstantinidis, and F. E. Löffler. 2021. Microbial taxonomy run amok.

827 Trends Microbiol. **29**: 394–404.

828 Schattenhofer, M., B. M. Fuchs, R. Amann, M. V. Zubkov, G. A. Tarran, and J. Pernthaler. 2009.

829 Latitudinal distribution of prokaryotic picoplankton populations in the Atlantic Ocean. Environ.

830 Microbiol. **11**: 2078–2093.

831 Schwalbach, M. S., H. J. Tripp, L. Steindler, D. P. Smith, and S. J. Giovannoni. 2010. The presence of the

832 glycolysis operon in SAR11 genomes is positively correlated with ocean productivity. Environ.

833 Microbiol. **12**: 490–500.

834 Shaiber, A. and others. 2020. Functional and genetic markers of niche partitioning among enigmatic

835 members of the human oral microbiome. Genome Biol. **21**: 292.

836 Sosa, O. A., D. J. Repeta, E. F. DeLong, M. D. Ashkezari, and D. M. Karl. 2019. Phosphate-limited ocean
837 regions select for bacterial populations enriched in the carbon-phosphorus lyase pathway for
838 phosphonate degradation. *Environ. Microbiol.* **21**: 2402–2414.

839 Sunagawa, S. and others. 2015. Ocean plankton. Structure and function of the global ocean microbiome.
840 *Science* **348**: 1261359.

841 Sun, J. and others. 2016. The abundant marine bacterium *Pelagibacter* simultaneously catabolizes
842 dimethylsulfoniopropionate to the gases dimethyl sulfide and methanethiol. *Nat Microbiol* **1**: 16065.

843 Sun, J., L. Steindler, J. C. Thrash, K. H. Halsey, D. P. Smith, A. E. Carter, Z. C. Landry, and S. J.
844 Giovannoni. 2011. One carbon metabolism in SAR11 pelagic marine bacteria. *PLoS One* **6**: e23973.

845 Suzuki, M. T., O. Béjà, L. T. Taylor, and E. F. Delong. 2001. Phylogenetic analysis of ribosomal RNA
846 operons from uncultivated coastal marine bacterioplankton. *Environ. Microbiol.* **3**: 323–331.

847 Thrash, J. C. and others. 2011. Phylogenomic evidence for a common ancestor of mitochondria and the
848 SAR11 clade. *Sci. Rep.* **1**: 13.

849 Thrash, J. C., B. Temperton, B. K. Swan, Z. C. Landry, T. Woyke, E. F. DeLong, R. Stepanauskas, and S.
850 J. Giovannoni. 2014. Single-cell enabled comparative genomics of a deep ocean SAR11 bathytype.
851 *ISME J.* **8**: 1440–1451.

852 Tripp, H. J., J. B. Kitner, M. S. Schwalbach, J. W. H. Dacey, L. J. Wilhelm, and S. J. Giovannoni. 2008.
853 SAR11 marine bacteria require exogenous reduced sulphur for growth. *Nature* **452**: 741–744.

854 Tsementzi, D. and others. 2016. SAR11 bacteria linked to ocean anoxia and nitrogen loss. *Nature* **536**:
855 179–183.

856 Tucker, S. J., K. C. Freel, A. M. Eren, and M. S. Rappe. 2024a. Habitat-specificity in SAR11 is associated
857 with a handful of genes under high selection. *bioRxiv*. doi:10.1101/2024.12.23.630198

858 Tucker, S. J., K. C. Freel, E. A. Monaghan, C. E. S. Sullivan, O. Ramfelt, Y. M. Rii, and M. S. Rappé.
859 2021. Spatial and temporal dynamics of SAR11 marine bacteria across a nearshore to offshore

860 transect in the tropical Pacific Ocean. *PeerJ* **9**: e12274.

861 Tucker, S. J., Y. M. Rii, K. C. Freel, K. Kotubetey, A. H. Kawelo, K. B. Winter, and M. S. Rappe. 2024b.

862 Sharp transitions in phytoplankton communities across estuarine to open ocean waters of the tropical

863 Pacific. *bioRxiv*. doi: 10.1101/2024.05.23.595464v1.

864 Tully, B. J., E. D. Graham, and J. F. Heidelberg. 2018. The reconstruction of 2,631 draft

865 metagenome-assembled genomes from the global oceans. *Sci Data* **5**: 170203.

866 Vergin, K. L. and others. 2013. High-resolution SAR11 ecotype dynamics at the Bermuda Atlantic

867 Time-series Study site by phylogenetic placement of pyrosequences. *ISME J.* **7**: 1322–1332.

868 Vergin, K. L., H. J. Tripp, L. J. Wilhelm, D. R. Denver, M. S. Rappé, and S. J. Giovannoni. 2007. High

869 intraspecific recombination rate in a native population of *Candidatus pelagibacter ubique* (SAR11).

870 *Environ. Microbiol.* **9**: 2430–2440.

871 Viklund, J., T. J. G. Ettema, and S. G. E. Andersson. 2012. Independent genome reduction and

872 phylogenetic reclassification of the oceanic SAR11 clade. *Mol. Biol. Evol.* **29**: 599–615.

873 Viklund, J., J. Martijn, T. J. G. Ettema, and S. G. E. Andersson. 2013. Comparative and phylogenomic

874 evidence that the alphaproteobacterium HIMB59 is not a member of the oceanic SAR11 clade. *PLoS*

875 *One* **8**: e78858.

876 Villarreal-Chiu, J. F., J. P. Quinn, and J. W. McGrath. 2012. The genes and enzymes of phosphonate

877 metabolism by bacteria, and their distribution in the marine environment. *Front. Microbiol.* **3**: 19.

878 Waite, D. W. and others. 2020. Proposal to reclassify the proteobacterial classes Deltaproteobacteria and

879 Oligoflexia, and the phylum Thermodesulfobacteria into four phyla reflecting major functional

880 capabilities. *Int. J. Syst. Evol. Microbiol.* **70**: 5972–6016.

881 Wang, Z., and M. Wu. 2013. A phylum-level bacterial phylogenetic marker database. *Mol. Biol. Evol.* **30**:

882 1258–1262.

883 Wick, R. R., L. M. Judd, C. L. Gorrie, and K. E. Holt. 2017. Unicycler: Resolving bacterial genome

884 assemblies from short and long sequencing reads. PLoS Comput. Biol. **13**: e1005595.

885 Wilhelm, L. J., H. J. Tripp, S. A. Givan, D. P. Smith, and S. J. Giovannoni. 2007. Natural variation in

886 SAR11 marine bacterioplankton genomes inferred from metagenomic data. Biol. Direct **2**: 27.

887 Yoshitake, K. and others. 2021. Development of a time-series shotgun metagenomics database for

888 monitoring microbial communities at the Pacific coast of Japan. Sci. Rep. **11**: 12222.

889 Zhao, J. and others. 2024. Promiscuous and unbiased recombination underlies the sequence-discrete

890 species of the SAR11 lineage in the deep ocean. bioRxiv. doi:10.1101/2024.10.30.621061

891

892

893

894

895

896

897

898

899

900

901

902

903 Supplemental Figures

904 All supplemental figures are available on FigShare at:

905 <https://doi.org/10.6084/m9.figshare.28087760>.

906

907

908

909

910

911

912

913

914

915

916

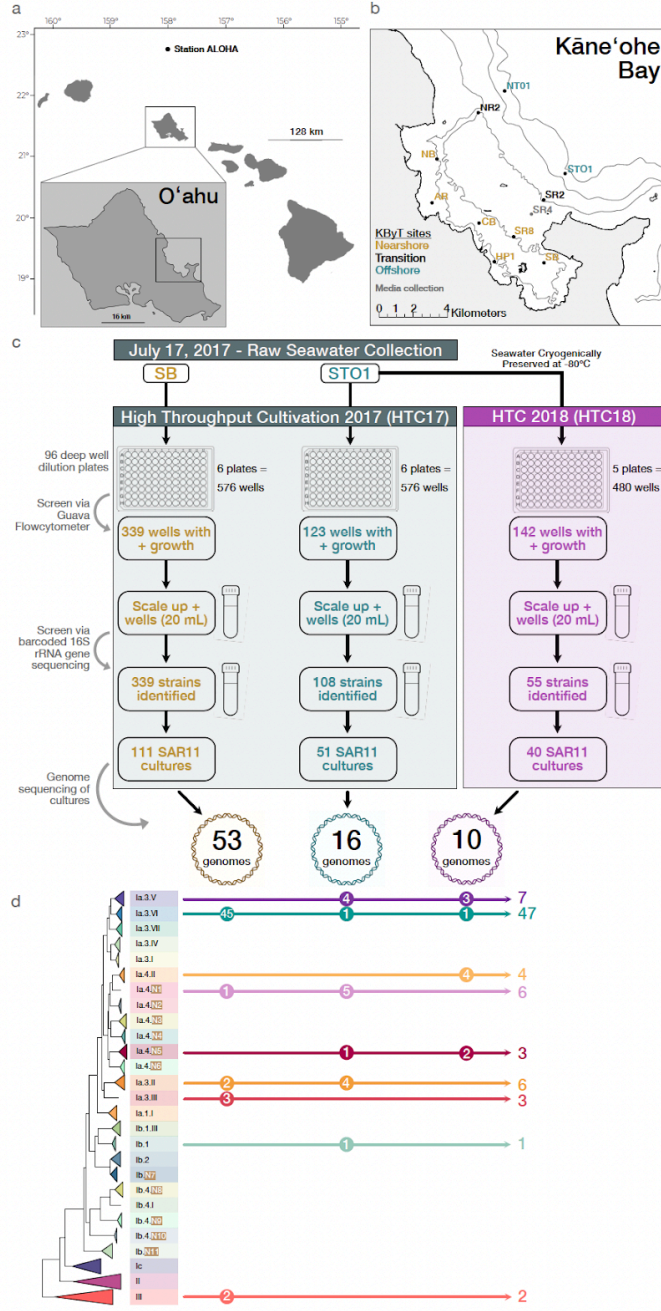
917

918

919

920

921



922

923 Supplemental Figure 1. Sampling sites used for high-throughput culturing experiments. (a)

⁹²⁴ Location of O'ahu in the Hawaiian archipelago in relations to Station ALOHA approximately

925 100 km north. **(b)** Map of the embayment on the windward side of O'ahu with sites included in

926 the Kāne'ohe Bay Time-series with sites classified as 'nearshore' (orange text), 'transition'

927 the same one-day time series with sites classified as 'nearshore' (orange text), 'transition'
927 (black text), or 'offshore' (turquoise text). Site SR4 in gray from which seawater media was

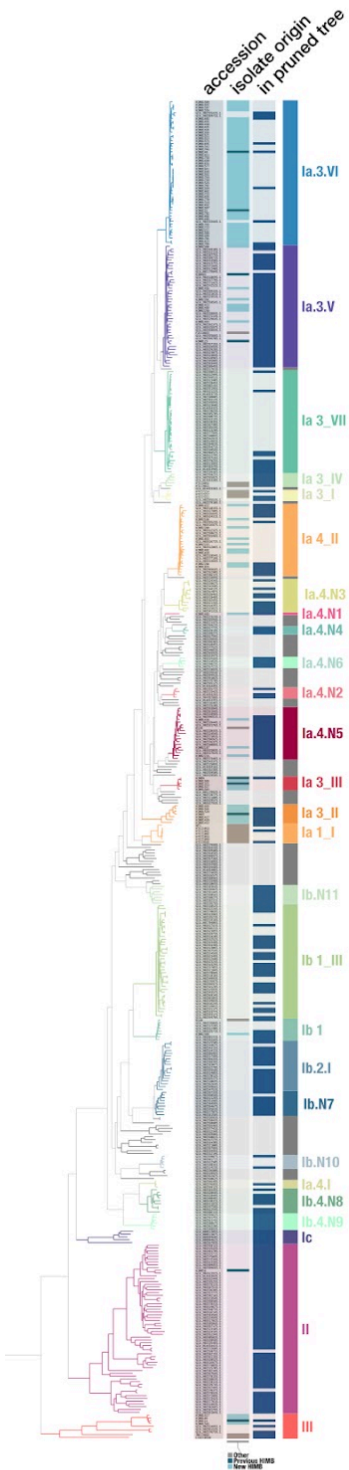
(black text), or onshore (turquoise text). Site SRY4 in gray from which seawater media was collected for the cultivation experiments is also indicated. Bathymetry lines are approximate (c).

Flowchart outlining the high-throughput cultivation (HTC) experiments conducted in 2017 and 2018 for the cultivation experiments is also indicated. Bathymetry lines are approximate. (C)

929 Flowchart outlining the high throughput cultivation (HTC) experiments conducted in 2017 and
930 2018 leading to the isolation of hundreds of SAB11 cultures and 79 new SAB11 isolate genomes.

930 2018 leading to the isolation of hundreds of SART1 cultures and 79 new SART1 isolate genotypes.

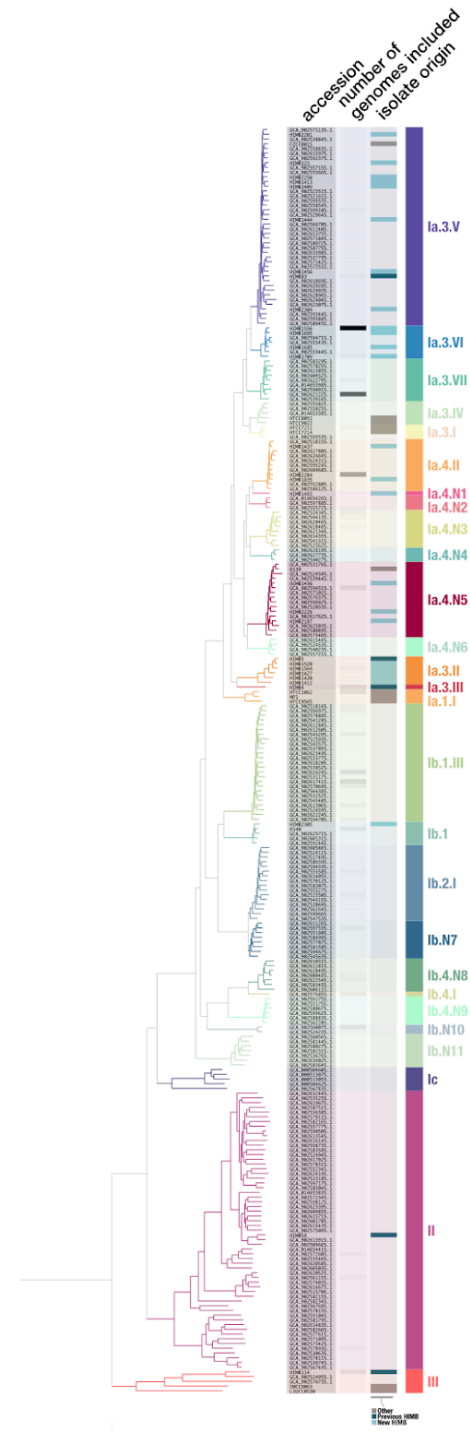
931 (d) Schema



933

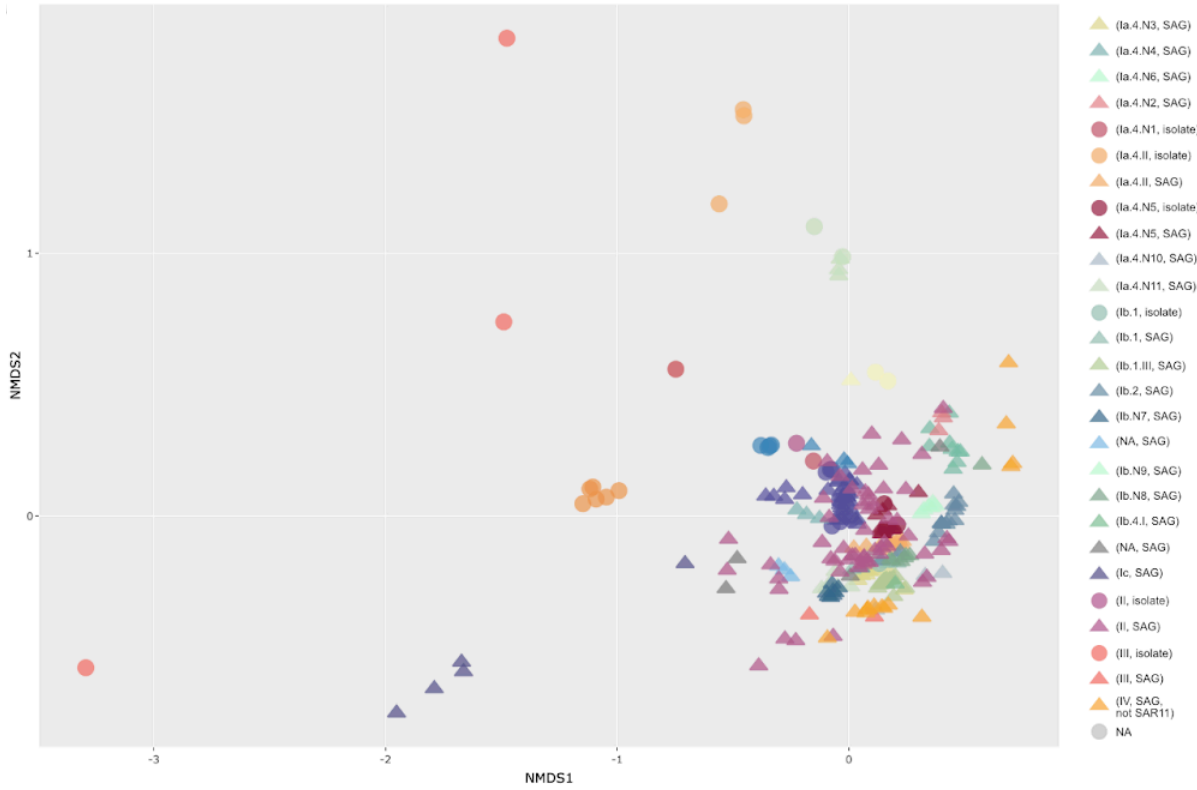
934

935 **Supplemental Figure 2. Phylogenomic tree of all 481 *Pelagibacterales* genomes initially
936 included.** Of the 481 SAR11 genomes 106 were isolates and 375 SAGs and the phylogeny is
937 based on a curated SAR11-specific set of 165 genes. Isolate origin is indicated and indicates if
938 the genome was from this study, a previous isolate from Kāne‘ohe Bay, or from another source.
939 Genomes included in the pruned tree are also indicated.



940

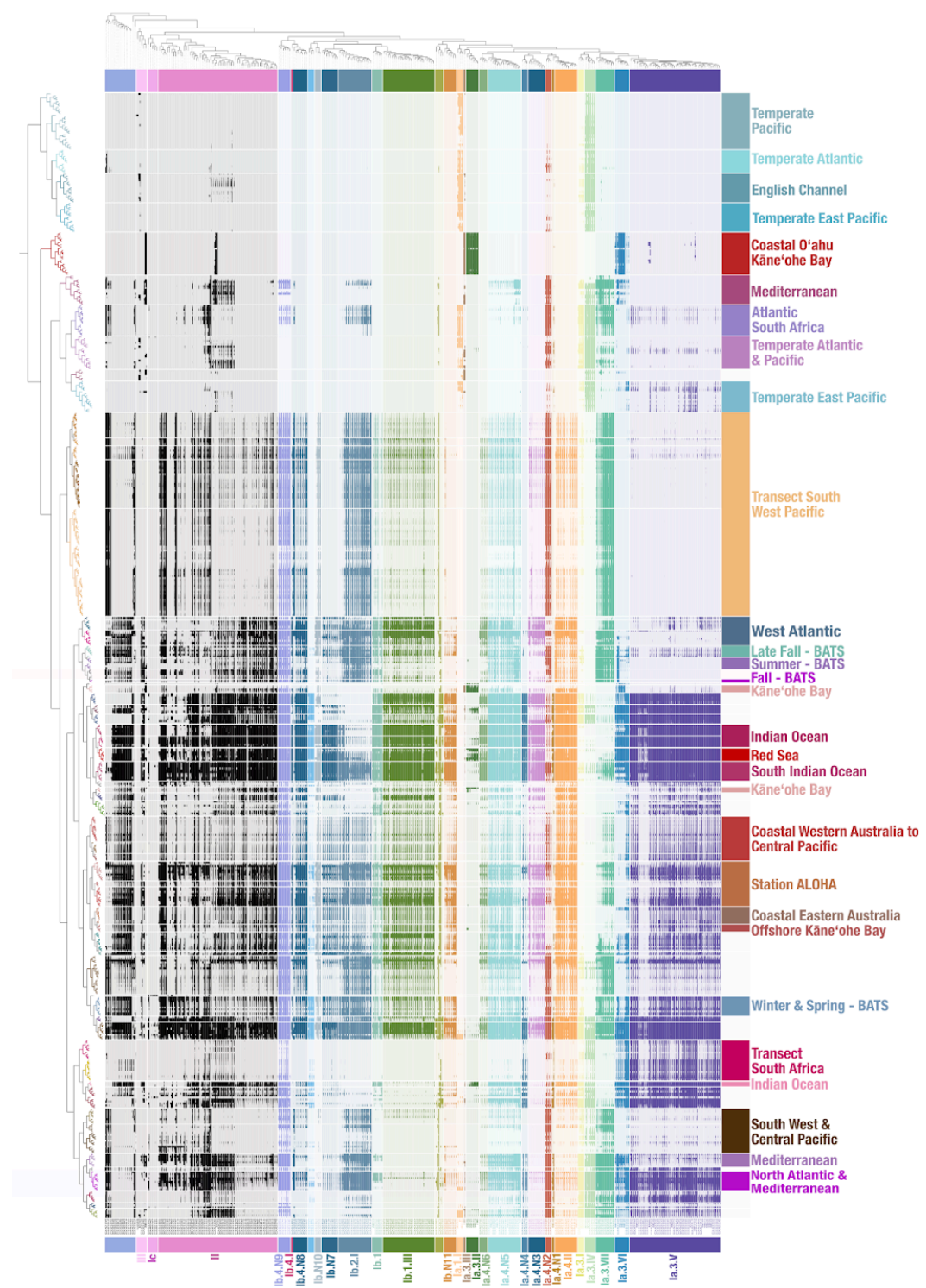
941 **Supplemental Figure 3. Pruned phylogenomic tree with 268 *Pelagibacterales* genomes.** Of
942 the 268 genomes 50 were isolates and 218 SAGs based on a curated SAR11-specific set of 165
943 genes. Isolate origin is highlighted on the tree and indicates if the genome was from this study, a
944 previous isolate from Kāne‘ohē Bay, or from another source. Number of additional genomes in
945 the same 95% gANI cluster are indicated as well by intensity of the bar which range from 0 to
946 45.



947

948 **Supplemental Figure 4. NMDS of genomes with detection data.** All of the genomes included
949 in the analysis are included here, with distinction between isolate genome (circle) or SAG
950 (triangle) indicated. Genomes not designated a subgroup noted as NA.

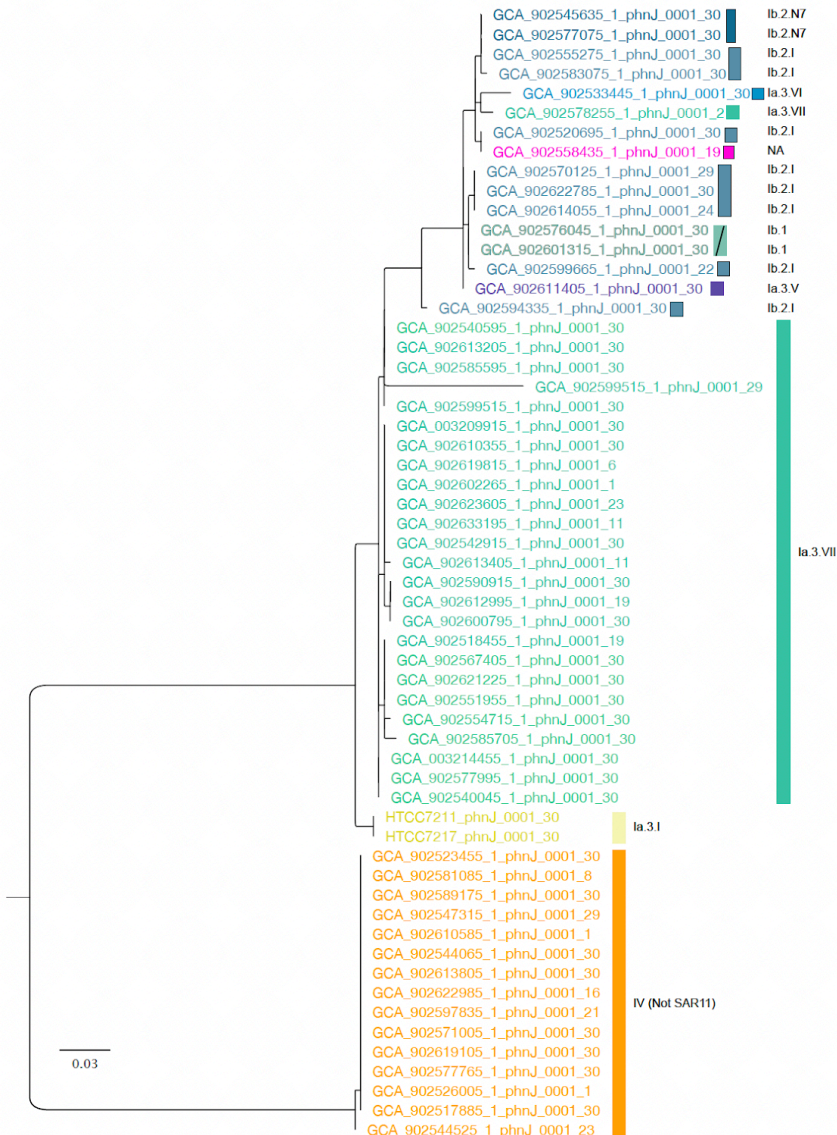
951



952

953

954 **Supplemental Figure 5. Read recruitment data including all metagenomes included in**
955 **cluster analysis of metagenomes based on genome detection values using the k-means**
956 **algorithm.** Subgroups are indicated at the bottom of the figure with labels indicating the
957 metagenome groups along the right hand side of the figure.



958

959 Supplemental Figure 6. Phylogeny of the *phnJ* gene for all *Pelagibacterales* genomes in the
960 pruned phylogeny data set.

961

962 Supplemental Table Legends

963 All supplemental tables are available on FigShare at:

964 <https://doi.org/10.6084/m9.figshare.28087490.v1>.

965

966 **Supplemental Table 1. Summary of the 16S rRNA gene amplicon data from HTC17 and**
967 **HTC18.**

968

969 **Supplemental Table 2. Detailed information for the isolate genomes reported in this study.**

970 The genome summary information originated from checkM (v1.1.2). *Indicates the genome has
971 been manually verified to be completely closed.

972

973 **Supplemental Table 3. Summary statistics for all genomes used for analyses in this study.**

974 This includes isolates reported here, previously published isolate genomes, and high-quality
975 single amplified genomes (SAGs) used in the extended SAR11 phylogeny. The genomes used in
976 read-recruitment are indicated. *Indicates the accession is the IMG Genome ID not the NCBI
977 Accession.

978

979 **Supplemental Table 4. Gene sets evaluated for use in SAR11 phylogenetics.** The sets
980 evaluated include the bac120 (Parks et al., 2018) and a subset of 165 of the genes (SAR11_165)
981 delineated for the Alphaproteobacteria (Wang and Wu 2013; Muñoz-Gómez, 2019).

982

983 **Supplemental Table 5. Summary of average genome statistics for the 23 genera established**
984 **in the *Pelagibacteraceae* as well as the Ic, II, and III families.**

985

986 **Supplemental Table 6. Studies from which metagenomes were sourced.**

987

988 **Supplemental Table 7. List of all metagenomes used for read recruitment and accession**
989 **numbers.**

990

991 **Supplemental Table 8. Detection values across genomes from all metagenomes used in read**
992 **recruitment.**

993

994 **Supplemental Table 9. Average detection across genome cluster for bins in Fig 3.**

995

996 **Supplemental Table 10. Coverage values across genomes from all metagenomes used in**
997 **read recruitment.**

998

999 Supplemental Table 11. Type genomes and classification hierarchy for the *Pelagibacterales*
1000 including proposed naming schemes.

1001

1002 Supplemental Table 12. All of the final 95% ANI clusters defined including the cluster
1003 number, the final representative genome for that cluster and the list of other genomes in the
1004 same cluster.